

Graph-Free Root Cause Analysis

Luan Pham¹

Abstract

Failures in complex systems demand rapid Root Cause Analysis (RCA) to prevent cascading damage. Existing RCA methods that operate without dependency graph typically assume that the root cause having the *highest anomaly score*. This assumption fails when faults propagate, as a small delay at the root cause can accumulate into a much larger anomaly downstream. In this paper, we propose **PRISM**, a simple and efficient framework for RCA when the dependency graph is absent. We formulate a class of component-based systems under which PRISM performs RCA with theoretical guarantees. On 735 failures across 9 real-world datasets, PRISM achieves 68% Top-1 accuracy, a 258% improvement over the best baseline, while requiring only 8ms per diagnosis.

1. Introduction

Modern IT systems drive critical infrastructure, from hospital services to financial markets. When these systems fail, rapid root cause identification determines whether operators can intervene before damage cascades. Delays may lead to significant economic losses (Yahoo, 2018), or even fatalities (Gregory, 2025). Root Cause Analysis (RCA) has thus attracted substantial research attention across domains (Orchard et al., 2025; Li et al., 2025; Jha et al., 2025; Pham et al., 2025; Zhang et al., 2025). Given a failure, RCA aims to identify the component whose mechanism changed and subsequently propagated its effects to other components.

Existing RCA approaches face a fundamental dichotomy. Methods that assume known structural dependencies reduce RCA to a traversal problem, where the root cause is a component with no anomalous parents (Budhathoki et al., 2022; Li et al., 2022; Xin et al., 2023). However, this knowledge is often unavailable in large, evolving systems. Methods that construct causal graphs from observational data using causal discovery techniques have also shown limited success. Pham et al. (2024b) evaluate twenty-one

causal inference-based RCA methods and conclude that they fall short, largely due to the limitations of causal discovery. Therefore, it is necessary to develop efficient RCA techniques without requiring structural dependency knowledge (Orchard et al., 2025; Pham et al., 2024a). This raises a fundamental question: **When the structural dependency graph is unknown, how can we determine the root cause?**

A natural alternative is to rank root cause candidates by their anomaly score, assuming that *the root cause exhibits the highest anomaly score* (Orchard et al., 2025; Pham et al., 2024a; Shan et al., 2019). For instance, Orchard et al. (2025) claim that “an anomaly x_i is unlikely to cause a much larger anomaly x_j anywhere downstream.” However, this assumption fails when faults propagate and amplify. Let’s consider a concrete fan-in pattern where a service calls a backend k times sequentially. If the backend experiences a small delay Δ , the service observes a cumulative delay of $k\Delta$. With $k > 1$, the downstream service appears more anomalous than the root cause, misleading score-based RCA methods.

Our key observation is that root causes and affected components exhibit a fundamental asymmetry. Root causes show anomalies in both internal properties (e.g., config states) and external properties (e.g., response latency, error rate). Affected components, by contrast, show anomalies only in external properties because faults propagate through observable interfaces, not through internal state. This asymmetry persists regardless of how severely downstream anomalies amplify. We formalize this insight through the Component-Property Model, which captures systems where internal properties causally precede external properties and inter-component influence occurs only through external channels. Building on this model, we introduce **PRISM**, a simple and efficient RCA framework that exploits this internal–external distinction. In summary, our key contributions are:

- We propose **PRISM**, a simple and efficient RCA framework that effectively localizes root causes of failures.
- We introduce the Component-Property Model, formalizing a class of systems with internal-external property decomposition. We show that, under this formulation, PRISM performs RCA with theoretical guarantees.
- We conduct extensive experiments on nine real-world datasets from RCAEval, comprising 735 failures. PRISM achieves 68% Top-1 accuracy, a 258% improvement over the best baseline, while requiring only 8ms per diagnosis.

¹RMIT University, Australia. Correspondence to: Luan Pham <luan.pham@rmit.edu.au>.

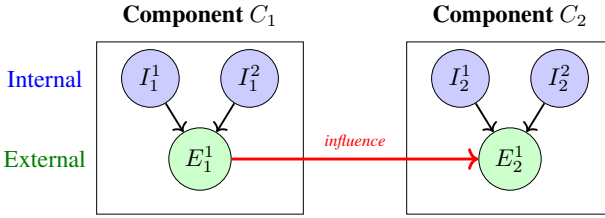


Figure 1. Component-Property Model. Solid arrows denote causal influence between **internal properties** (e.g., configs) and **external properties** (e.g., response time). Faults originate in internal properties and propagate through external properties (Axioms 2.5–2.6).

2. Component-Property Model

A key challenge in RCA is to distinguish the root cause from affected components. When faults propagate, downstream anomalies can exceed upstream ones, making score-based ranking unreliable. To address this, we introduce the Component-Property Model, which formalizes a class of systems where internal and external properties are explicitly decomposed. This decomposition enables PRISM to identify root causes without requiring a dependency graph.

Definition 2.1. A **component-based system** is a triple $\mathcal{S} = (\mathcal{C}, \mathcal{I}, \mathcal{E})$ where $\mathcal{C} = \{C_1, \dots, C_n\}$ is a set of n components. $\mathcal{I} = \bigcup_{i=1}^n \mathbf{I}_i$ is the set of all internal properties, where $\mathbf{I}_i = \{I_i^1, \dots, I_i^{k_i}\}$ are internal properties of component C_i . $\mathcal{E} = \bigcup_{i=1}^n \mathbf{E}_i$ is the set of all external properties, where $\mathbf{E}_i = \{E_i^1, \dots, E_i^{m_i}\}$ are external properties of C_i .

Definition 2.2. Internal properties \mathbf{I}_i are local to component C_i and not directly observable by other components. Each $I_i^k \in \mathbf{I}_i$ is a real-valued observable (e.g., resource utilization, queue length, internal state variables).

Definition 2.3. External properties \mathbf{E}_i of component C_i are observable by other components through interactions. Each $E_i^l \in \mathbf{E}_i$ is a real-valued observable. External properties can causally influence external properties of other components. For example, high latency in component C_i may cause high latency in C_j if C_j depends on C_i .

The described component-based system, with its internal and external properties gives an abstraction of interconnected systems. In such systems, internal properties characterize how a component operates locally, whereas external properties describe the measurable outcomes of these operations as perceived by other components. Changes to a component’s internal property may give rise to externally observable behavior. Although causal relationships exist both within and across components, we assume: (1) a directional asymmetry between internal and external properties within each component (Axiom 2.5), and (2) inter-component causal influences occur only through external properties (Axiom 2.6). This abstraction allows PRISM to perform RCA without relying on an dependency graph.

Assumption 2.4 (Diagnostic Sufficiency). The pre- and post-failure observational data is sufficient to determine the

root cause. First, the root cause component is instrumented with at least one internal and one external property. Second, faults manifest in these properties. Third, no unmeasured external factors confound the observed anomalies.

Diagnostic sufficiency requires that the root cause component exhibits detectable anomalies in its properties. We term this *fault manifestation*. Specifically, if C_r is the root cause, properties of C_r must exhibit a detectable deviation from normal behavior. This manifestation can be quantified via anomaly scoring. Unlike [Orchard et al. \(2025\)](#) and [Pham et al. \(2024a\)](#), we do not assume the root cause has the highest anomaly score. The challenge is to determine, among all anomalous components, which component is the root cause.

Axiom 2.5 (Intracomponent). Internal properties are causal ancestors of external properties and there are no edges from external to internal properties within the same component.

The Axiom 2.5 captures a fundamental asymmetry between internal and external properties in component-based systems. Internal properties represent the internal states of a component (e.g., configurations, resource usage). External properties (e.g., latency, error rate) are observable outcomes of these internal states and therefore arise as their effects.

Axiom 2.6 (Intercomponent Isolation). Causal influences between different components occur through external properties. Formally, for any $i \neq j$, there are no direct causal edges from any property of C_i to internal properties of C_j .

In component-based software systems, components interact through well-defined interfaces. One component cannot directly alter another component’s internal state variables (e.g., resource allocation, configuration). The only causal pathway between components is through observable external properties (e.g., response time, error rate). For a detailed discussion of systems satisfying these Axioms 2.5–2.6 and practical applicability guidance, see Appendix D.2.3.

3. PRISM: Our Proposed Approach

Given the pre- and post-failure observational data, PRISM ranks candidate root causes based on a simple principle: *the root cause exhibits substantial anomalies in both internal and external properties, while downstream affected components show only external anomalies due to fault propagation*. Figure 2 gives an overview of PRISM pipeline, including anomaly scoring, score pooling, and root cause ranking.

3.1. Anomaly Scoring

Anomaly scoring is foundational to RCA as all downstream reasoning depends on how deviations from normal behavior are quantified. We identify two conditions that a scorer must satisfy for reliable RCA: *monotonicity* and *injectivity*.

An anomaly scorer is a function $S : \mathcal{X} \rightarrow \mathbb{R}_{\geq 0}$. We adopt *deviation-based anomaly scoring*, which directly measures

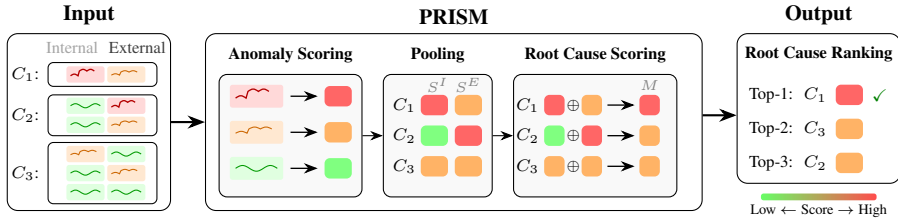


Figure 2. Overview of PRISM. Given observational data of internal and external properties for each component, PRISM first computes deviation-based anomaly scores, then pools property-level scores into component-level internal (S_i^I) and external (S_i^E) scores, and finally ranks root cause components. The root cause (C_1) exhibits substantially high anomaly scores for both internal and external properties.

how far an observation departs from a reference baseline.

Definition 3.1. A *deviation-based anomaly scorer* is a function: $S(x; \theta) = \frac{|x - c(\theta)|}{s(\theta)}$, where $c(\theta)$ is a location parameter and $s(\theta) > 0$ is a scale parameter, both estimated from reference data with parameters θ . Examples include z-score (Orchard et al., 2025) or IQR-based score (Pham et al., 2024a).

For RCA, an anomaly scorer must preserve meaningful distinctions between deviation magnitudes, i.e., if one component deviates more than others, it should receive a higher score. We formalize this requirement through two conditions. *Monotonicity* ensures larger deviations yield larger scores. *Injectivity* ensures distinct deviations receive distinct scores, preventing ties that would make ranking impossible.

Definition 3.2 (Monotonicity). An anomaly scoring function S is *monotonic* if larger deviations yield larger scores:

$$|x - c| > |y - c| \implies S(x) > S(y). \quad (1)$$

Definition 3.3 (Injectivity). A scorer S is *injective* if it assigns distinct scores to observations with distinct deviations:

$$|x_i - c| \neq |x_j - c| \implies S(x_i) \neq S(x_j), \quad \forall i \neq j. \quad (2)$$

Lemma 3.4. *Monotonicity (Definition 3.2) implies injectivity (Definition 3.3). The converse does not hold in general.*

Theorem 3.5 (Deviation-based Scorers satisfy conditions). *Let S be a deviation-based anomaly score as in Definition 3.1. Then S is monotonic and injective.*

The proof is straightforward (see Appendix A). This result establishes that simple deviation-based scorers (z-scores, IQR-scores) are provably suitable for RCA, with both conditions following directly from the linear relationship between deviation magnitude and anomaly score.

Having established that deviation-based scores satisfy these conditions, we now show that injectivity is necessary.

Theorem 3.6. *Let S be an anomaly scoring function. If S is not injective, then there exist failure scenarios where S cannot solve the RCA ranking problem.*

If S assigns equal scores to distinct deviations, the root cause and affected components may receive identical scores

despite different anomaly magnitudes, making correct ranking impossible. See Appendix A for the complete proof.

This result explains why certain scorers fail at RCA. For example, Information-Theoretic (IT) scorers violate injectivity when post-fault observations exceed the reference distribution. We analyze this problem empirically in Section C.2.

3.2. Score Pooling

We now pool property-level anomaly scores into component-level scores as different components may expose different numbers of properties depending on their specific instrumentation. A component with many properties should not necessarily outrank one with few. We therefore pool property-level scores into a single internal score S_i^I and a single external score S_i^E for each component C_i .

Definition 3.7 (Score Pooling). A *pooling function* $\phi : \mathbb{R}_{\geq 0}^n \rightarrow \mathbb{R}_{\geq 0}$ aggregates property-level anomaly scores into a component-level score. For each component C_i :

$$S_i^T = \phi(\{S(P) : P \in \mathbf{T}_i\}), \quad T \in \{I, E\}.$$

To preserve semantics, ϕ must satisfy two conditions. First, ϕ must be monotonic (Definition 3.2), i.e., increasing any property-level score must not decrease the pooled score. This ensures that anomaly evidence is never suppressed during pooling. Second, ϕ must be permutation-invariant.

Definition 3.8 (Permutation Invariance). A pooling function ϕ is *permutation-invariant* if for any permutation π ,

$$\phi(x_1, \dots, x_n) = \phi(x_{\pi(1)}, \dots, x_{\pi(n)}).$$

Common aggregators (max, mean, and sum) satisfy both conditions. We empirically show in Section 4.4 that PRISM is effective and robust across these choices. The pooled scores S_i^I and S_i^E now serve as inputs to root cause ranking.

3.3. Root Cause Ranking

Given pooled scores S_i^I and S_i^E for each component C_i , we rank components to identify the root cause. The key insight is that the root cause exhibits anomalies in *both* internal and external properties, while affected components show anomalies only in external properties.

Let $M : \mathbb{R}_{\geq 0}^2 \rightarrow \mathbb{R}_{\geq 0}$ combine internal and external scores into a root cause score. To ensure correct ranking, M must satisfy two conditions: (1) *monotonicity* in both arguments

(Definition 3.2), ensuring that stronger anomaly evidence yields higher scores; and (2) *internal boundedness*:

Definition 3.9 (Internal Boundedness). A scoring function M satisfies *internal boundedness* if there exists a monotonically increasing $f : \mathbb{R}_{\geq 0} \rightarrow \mathbb{R}_{\geq 0}$ such that $M(s^I, s^E) \leq f(s^I)$ for all $s^I, s^E \geq 0$.

Internal boundedness ensures that a component's overall score is controlled by its internal anomaly score, regardless of external score magnitude. When s^I is at nominal level (i.e., consistent with the pre-fault reference distribution), the bounding function $f(s^I)$ constrains M to be small, preventing affected components from outranking the root cause due to *amplified* external anomalies. The root cause, by contrast, has high scores for *both* internal and external properties.

We now present two scorers satisfying these requirements:

Additive Score. When both internal and external evidence should contribute additively, we use:

$$M_{\text{add}}(C_i) = S_i^I + S_i^E - \log(1 + S_i^I + S_i^E) \quad (3)$$

The additive score M_{add} treats anomalies in internal and external properties as cumulative evidence, summing both contributions while applying a logarithmic correction to prevent any single source from dominating the final ranking.

Proposition 3.10. M_{add} satisfies monotonicity. Under bounded external amplification (i.e., $S^E \leq \alpha \cdot S^I + \beta$ for constants α, β), it satisfies internal boundedness.

Conjunctive Score. An alternative is to require *both* internal and external evidence to be high, taking their minimum:

$$M_{\text{conj}}(C_i) = \min(S_i^I, S_i^E) \quad (4)$$

The conjunctive score M_{conj} adopts a more conservative stance by taking the minimum of internal and external scores, thereby requiring *both* sources of evidence to be elevated before assigning a high root cause score. It provides unconditional stronger guarantees against external anomaly amplification, at the cost of potentially underweighting components with asymmetric anomaly patterns.

Proposition 3.11. M_{conj} satisfies monotonicity and internal boundedness with $f(s) = s$. See Appendix A for proofs.

Both scorers satisfy the requirements for correct ranking (Theorem 3.13). The additive score offers finer score separation when external amplification is bounded, while the conjunctive score provides unconditional guarantees against arbitrary amplification. In Section 4.4, we show that both of them achieve comparable empirical performance.

Theoretical Guarantee. The correctness of PRISM rests on the separation between root cause and affected components, i.e., faults originate in internal properties and propagate only through external properties.

Lemma 3.12. Under Axioms 2.5 and 2.6, suppose a fault originates in an internal property of component C_r (the root cause). Let C_a be any affected component. Then:

1. $S^I(C_r) \geq S(I_r^k) > 0$ for some anomalous $I_r^k \in \mathbf{I}_r$
2. $S^I(C_a)$ remains at nominal levels
3. Under Assumption 2.4, $S^I(C_r) > S^I(C_a)$

Theorem 3.13. Let M satisfy monotonicity and internal boundedness. If the root cause exhibits anomalies in both internal and external properties, while affected components exhibit anomalies only in external properties, then $M(C_r) > M(C_a)$ for any affected component C_a .

Why Not Rank by Internal Score Alone? If the root cause has high internal anomaly score, why not rank by S^I alone? Relying solely on internal scores requires a strong form of Assumption 2.4, i.e., the fault must manifest with sufficient magnitude in internal properties to enable correct ranking. In practice, this may not hold. A code bug in microservices, for instance, may not produce a detectable spike in resource metrics. By incorporating external properties, PRISM relaxes this assumption, i.e., even when internal anomalies are weak, the combination of internal and external scores can still help to distinguish the root cause candidates from affected components, whose properties are at nominal levels.

4. Evaluation

In this section, we conduct comprehensive experiments primarily aimed at answering the following research questions:

RQ1: How effective is PRISM?

RQ2: How efficient is PRISM?

RQ3: How robust is PRISM?

RQ4: What is the contribution of each PRISM component?

4.1. Experimental settings

4.1.1. DATASETS

We evaluate PRISM on nine datasets in RCAEval benchmark (Pham et al., 2025), comprising 735 failure cases. The datasets are collected from three microservice systems (Online Boutique, Sock Shop, and Train Ticket), containing 11 to 64 interacting components. The dataset contains multimodal data with 11 fault types (4 resource faults, 2 network faults, and 5 code-level faults) with annotated root cause. Table 1 summarizes the dataset statistics.

Internal-External Property Decomposition. We classify properties based on their observability to other components (Li et al., 2022; Google, 2024). External properties are observable metrics at component boundaries including response time and error rate. Internal properties are local resource states: CPU usage, memory utilization, disk I/O, and socket count. We further validate this classification empirically and link to previous works in Appendix D.

4.1.2. BASELINES

We compare PRISM against eight state-of-the-art RCA methods, covering a wide range of approaches, including:

Table 1. Statistics of the nine RCAEval benchmark datasets.

System	Dataset	#Components	#Properties	#Faults	#Cases
Online Boutique	RE1OB	12	49	5	125
	RE2OB	12	72	6	90
	RE3OB	12	69	5	30
Sock Shop	RE1SS	13	59	5	125
	RE2SS	13	75	6	90
	RE3SS	13	80	4	30
Train Ticket	RE1TT	64	220	5	125
	RE2TT	64	369	6	90
	RE3TT	64	315	4	30
Total		12-64	49-369	11	735

Methods that do NOT require structural knowledge:

- ▷ **BARO** (Pham et al., 2024a) uses a IQR-based anomaly scorer to analyse pre- and post-failure observational data. BARO ranks the most anomalous property as root cause.
- ▷ **ScoreOrdering** (Orchard et al., 2025) uses an Information-theoretic (IT) Anomaly Scorer and rank the component that has highest anomaly score as root cause.
- ▷ **Cholesky** (Li et al., 2025) uses the Cholesky decomposition of the covariance matrix of observational data, exploiting permutation invariance to identify the root cause.
- ▷ **PcPageRank** (Pham et al., 2025) constructs a causal graph from observational data using PC algorithm. Then, it uses PageRank to find the root cause, assuming the root cause affects other components during the failure time.

Methods that require structural knowledge:

- ▷ **Counterfactual** (Hardt et al., 2024) finds the Shapley contribution of each property to the target property and outputs the one with the highest contribution as root cause.
- ▷ **RCLAgent** (Zhang et al., 2025) uses LLMs to recursively traversing and analysing anomalous components along the topology graph constructed from traces.
- ▷ **Traversal** (Orchard et al., 2025) identifies nodes which are anomalous, have no anomalous parents, and are linked to the target node via a path in the constructed graph.
- ▷ **SmoothTraversal** (Orchard et al., 2025) is an improvement of Traversal, incorporating IT anomaly scoring, anomalous parents, and are linked to the target node via a path of anomalous nodes as root causes.

For all baselines, we follow the recommendations in their papers to set their hyperparameters. For methods with configurable thresholds, we follow established practice by running multiple settings and reporting the best performance.

Retrieving Structural Knowledge. The RCAEval benchmark does not provide the structural dependency graph. In order to run the baselines that require this graph, we engage a DevOps engineer to deploy the systems used in RCAEval, and instrument them to capture interaction between components (i.e., services). Note that while this instrumentation capture the structural knowledge, the latency overhead is confirmed significant. We release this data in our package.

4.1.3. EVALUATION METRICS

We use two standard evaluation metrics: Top@ k and Avg@ k to measure the RCA performance. Given a set of failure cases A , Top@ k is calculated as follows,

$$\text{Top}@k = \frac{1}{|A|} \sum_{a \in A} \frac{\sum_{i < k} R^a[i] \in V_{rc}^a}{\min(k, |V_{rc}^a|)}, \quad (5)$$

where $R^a[i]$ is the i th ranking result for the failure case a by an RCA method, and V_{rc}^a is the true root cause set of case a . Top@ k represents the probability the top k results of the given method include the true root causes. Its values range from 0 to 1, with higher values indicating better performance. Avg@ k , which shows the overall RCA performance, is measured as $\text{Avg}@k = \frac{1}{k} \sum_{j=1}^k \text{Top}@j$.

To assess whether performance differences are meaningful, we employ the paired Wilcoxon signed-rank test with Holm-Bonferroni correction (McDonald, 2014). When comparing PRISM against k baselines, we apply Holm-Bonferroni correction to control the family-wise error rate at $\alpha=0.05$. In our tables, we denote (+) to indicate PRISM performs significantly better than the baseline, (-) to indicate significantly worse, and (\approx) for no significant difference.

Table 2. Overall Performance on Nine Tested Datasets.

Method	AVERAGE			STAT
	Top-1	Top-3	Avg@5	
Counterfactual	0.07	0.12	0.12	$1.2e^{-112(+)}$
RCLAgent	0.10	0.18	0.16	$5.4e^{-39(+)}$
Smooth-Traversal	0.05	0.19	0.16	$1.3e^{-113(+)}$
PC-PageRank	0.09	0.21	0.21	$3.9e^{-110(+)}$
Cholesky	0.09	0.22	0.22	$1.7e^{-107(+)}$
Simple-Traversal	0.09	0.24	0.22	$3.1e^{-108(+)}$
Score-Ordering	0.11	0.30	0.29	$8.6e^{-101(+)}$
BARO	0.19	0.74	0.63	$1.3e^{-61(+)}$
PRISM	0.68	0.91	0.87	N/A

4.2. Effectiveness in RCA

To answer RQ1, we evaluate PRISM against eight state-of-the-art baselines on nine datasets from the RCAEval benchmark, a total of 735 failure cases. Tables 2 and 3 present the overall results and the detailed results on the RE2OB dataset, respectively. Due to space limitations, we put the detailed results for other datasets in Appendix C.1.

Overall Performance. Table 2 summarizes the overall performance across all 735 failure cases over nine datasets in the RCAEval benchmark. PRISM achieves 68% Top-1 accuracy, substantially outperforming the second-best method BARO (19%), a relative improvement of 258% (from 19% to 68%). The improvement persists across all metrics. PRISM achieves 91% Top-3 and 87% Avg@5, compared to 74% and 63% for BARO respectively. All improvements are statistically significant. These results demonstrate that PRISM can reliably identify the root cause

Table 3. RCA Method Performance on RE2OB (Online Boutique with multimodal data)

Method	CPU			DELAY			DISK			LOSS			MEM			SOCKET			AVERAGE			STAT	
	Top-1	Top-3	Avg@5																				
Simple-Traversal	0.07	0.13	0.12	0.00	0.13	0.12	0.00	0.07	0.05	0.07	0.13	0.16	0.13	0.13	0.17	0.00	0.13	0.11	0.04	0.12	0.12	$7.9e^{-17}_{(+)}$	
Smooth-Traversal	0.07	0.13	0.11	0.00	0.07	0.07	0.00	0.13	0.12	0.07	0.20	0.19	0.07	0.33	0.24	0.00	0.20	0.13	0.03	0.18	0.14	$9.1e^{-17}_{(+)}$	
PC-PageRank	0.00	0.20	0.23	0.13	0.20	0.24	0.00	0.07	0.09	0.00	0.13	0.13	0.00	0.07	0.08	0.00	0.20	0.12	0.02	0.14	0.15	$2.0e^{-16}_{(+)}$	
Counterfactual	0.00	0.20	0.15	0.20	0.27	0.24	0.13	0.27	0.24	0.07	0.13	0.13	0.13	0.13	0.13	0.13	0.13	0.13	0.11	0.19	0.17	$7.7e^{-16}_{(+)}$	
Cholesky	0.07	0.13	0.16	0.07	0.13	0.17	0.13	0.27	0.23	0.07	0.07	0.13	0.16	0.07	0.13	0.16	0.07	0.27	0.25	0.08	0.17	0.18	$9.7e^{-16}_{(+)}$
RCLAgent	<u>0.20</u>	0.20	0.20	0.07	<u>0.33</u>	0.28	0.13	0.27	0.23	0.27	0.47	0.41	0.27	<u>0.40</u>	0.35	<u>0.13</u>	0.27	0.27	0.18	0.32	0.29	$1.6e^{-14}_{(+)}$	
Score-Ordering	0.07	0.20	0.21	0.00	0.13	0.12	0.07	0.27	0.36	0.20	0.33	0.36	0.07	0.20	0.25	0.00	0.33	0.41	0.07	0.24	0.29	$2.9e^{-15}_{(+)}$	
BARO	0.07	0.87	<u>0.71</u>	0.13	0.80	<u>0.68</u>	0.80	1.00	<u>0.96</u>	<u>0.47</u>	<u>0.87</u>	<u>0.80</u>	<u>0.53</u>	1.00	<u>0.88</u>	0.07	<u>0.87</u>	<u>0.68</u>	<u>0.34</u>	0.90	<u>0.78</u>	$6.5e^{-12}_{(+)}$	
PRISM	0.87	1.00	0.97	0.80	0.80	0.88	1.00	1.00	1.00	0.93	0.92	1.00	1.00	1.00	0.93	1.00	0.99	0.90	0.96	0.96	N/A		

as its top prediction in the majority of cases, whereas existing methods require examining multiple candidates.

Finding 1: PRISM consistently outperforms all baselines, achieves **68% Top-1 accuracy** overall, outperforming the best baseline by 258%. The internal-external decomposition provides a fundamentally more effective signal than marginal anomaly scoring.

Performance by Fault Type. Table 3 presents the detailed results across different fault types in the RE2OB dataset. We observe that PRISM excels across different fault types. For resource faults, PRISM achieves perfect accuracy of 100% Top-3 across CPU, MEM, DISK, and SOCKET faults. These faults directly corrupt internal properties (resource metrics), which PRISM’s internal-external decomposition is designed to detect. Network faults (DELAY, LOSS) are more challenging. PRISM achieves 80%–93% Top-3 accuracy respectively, yet still substantially outperforms all other baselines. The lower accuracy on DELAY faults reflects the inherent difficulty in diagnosing failures as network delays may not immediately manifest in internal resource metrics.

Finding 2: PRISM achieves 100% Top-3 accuracy on resource faults (CPU, MEM, DISK, SOCKET) where faults directly corrupt internal properties. Network faults (DELAY, LOSS) achieve 80–93% Top-3 accuracy as they may not immediately manifest in resource metrics. PRISM outperforms all baselines in overall.

Why Do Baselines Fail? Existing methods fail due to fundamental limitations. IT-score-based methods (Score-Ordering, Smooth-Traversal) suffer from *saturation* (Section C.2). When multiple components exhibit anomalies exceeding historical bounds, they receive identical scores, preventing discrimination. Methods based on marginal score ordering (BARO, Cholesky) assume the root cause exhibits the highest anomaly score. Theorem C.3 shows this assumption fails in fan-in scenarios where downstream effects exhibit larger anomalies than the root cause. BARO’s strong Top-3 (74%) but weak Top-1 (19%) confirms this pattern. The root cause is often among top candidates but not ranked first. Graph-based methods (PC-PageRank) achieve only 9% Top-1 accuracy, reflecting the difficulty of accurate causal discovery from observational data during failures (Pham

et al., 2024b). RCLAgent, despite leveraging topology knowledge, achieves only 10% Top-1. The bounded recursive exploration cannot systematically analyze the volume of trace data required for reliable diagnosis.

Finding 3: Existing methods fail due to (1) IT-score saturation violating injectivity, (2) invalid assumption that root causes exhibit highest anomaly scores, or (3) inability to process observational data at scale.

Failure Case Analysis. We analyze a disk fault in *currencyervice* of the Online Boutique system to illustrate how score-based methods can misrank propagated effects above true root causes. Table 4 shows BARO’s top-4 ranked candidates. The highest-scoring candidate is *emailservice-latency*, an external property of a downstream service, with score 4.6×10^{14} . The true root cause (*currencyervice*) appears at both rank 2 (*diskio*) and rank 4 (*latency*), exhibiting anomalies in both internal and external properties. Notably, the *emailservice* score dominates others substantially.

Table 4. BARO’s root cause ranking for a disk fault in *currencyervice*. The true root cause appears at ranks 2 and 4.

Rank	Root Cause Candidate	Anomaly Score
1	<i>emailservice-latency</i>	4.6×10^{14}
2	<i>currencyervice-diskio</i>	5.1×10^9
3	<i>redis-diskio</i>	5.0×10^4
4	<i>currencyervice-latency</i>	353.6

This analysis illustrates two key insights. First, *the highest anomaly score does not indicate the root cause*, i.e., the top candidate may be a propagated effect, not the root cause. Second, *internal-external decomposition distinguishes root causes from affected components*, as true root causes exhibit anomalies in both property types, while downstream services show only external anomalies. PRISM leverages this distinction. It ranks *currencyervice* first with score 141.1, while *emailservice*, despite its large external anomaly, receives a low score due to the absence of internal deviation.

4.3. Efficiency in RCA

To answer RQ2, we measure the running time of each RCA method across all 735 failure cases. In real-world environments, RCA must complete quickly to enable timely response. Figure 3 shows the runtime distribution per case.

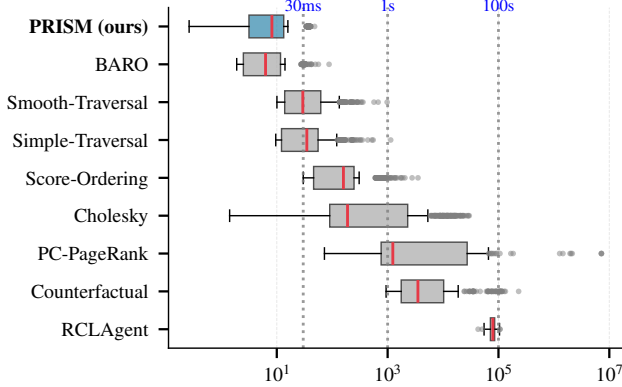


Figure 3. Running time per failure case (log scale). PRISM (8.2ms median) matches the efficiency of the fastest baseline (BARO).

Runtime Performance. PRISM achieves a median inference time of 8.2 milliseconds per case, making it the second-fastest after BARO (6.3ms). Both methods complete most diagnoses in under 15 milliseconds. In contrast, methods requiring causal graph construction or LLM inference incur substantially higher latency. PC-PageRank has a median of 1.2 seconds due to the computational cost of causal discovery. RCLAgent requires 79 seconds per case for LLM inference. Compared to these, PRISM is $146\times$ faster than PC-PageRank and $9,600\times$ faster than RCLAgent.

Efficiency-Effectiveness Tradeoff. The efficiency results reveal a favorable tradeoff for PRISM. Compared to BARO, PRISM provides 258% better Top-1 accuracy (Section 4.2) while incurring only 30% additional runtime, a negligible cost of 1.9 milliseconds. Cholesky and Counterfactual achieve comparable effectiveness to BARO but require significantly longer execution times (189ms and 3.5s median, respectively). Despite this additional computational cost, both methods still underperform PRISM.

Finding 4: PRISM requires only 8.2ms per diagnosis, incurring just 30% overhead compared to the fastest baseline (BARO). This modest overhead yields 258% improvement in Top-1 accuracy.

4.4. Robustness Analysis

We analyze the robustness of PRISM in two parts. First, we examine its robustness w.r.t different design choices. Second, we examine its sensitivity w.r.t different input lengths.

Different Anomaly Scorers. We evaluate four anomaly scorers: z-score and IQR-based score (deviation-based, satisfying Theorem 3.5), and their IT-wrapped variants (IT-zscore, IT-IQR). Table 5 shows that deviation-based scorers achieve 65–68% Top-1 accuracy, while IT-based variants degrade to 13–14%. This performance gap confirms our theoretical analysis. IT-scores violate injectivity (Theorem 3.6) due to saturation (Section C.2), assigning identical scores to components with vastly different anomaly magnitudes.

Finding 5: Deviation-based anomaly scorers (e.g., z-score, IQR-based score) performs significantly better than IT-based scorers, confirming that injectivity is necessary for reliable RCA (Theorem 3.6).

Different Pooling Strategies. We evaluate three pooling functions satisfying Definition 3.7: max (worst deviation), sum (total anomaly evidence), and mean (average deviation). Table 5 shows all three achieve comparable performance (68–69% Top-1). This robustness follows from the theoretical guarantees. Any monotonic, permutation-invariant aggregator preserves the ranking semantics for RCA.

Finding 6: PRISM is robust to the three tested pooling functions. Common monotonic, permutation-invariant aggregators (max, sum, mean) yield comparable performance, confirming PRISM’s robustness.

Table 5. Robustness of PRISM w.r.t Different Design Choices

Category	Variant	Top-1	Top-3	Top-5	Avg@5	Time (ms)
Anomaly	zscore [†]	0.68	0.91	0.98	0.87	12.6
	IQR	0.65	0.80	0.85	0.78	16.2
Scoring	IT-zscore	0.14	0.51	0.75	0.48	35.9
	IT-IQR	0.13	0.48	0.72	0.45	35.7
Score Pooling	max [†]	0.68	0.91	0.98	0.87	12.6
	sum	0.69	0.93	0.98	0.89	13.2
	mean	0.68	0.92	0.98	0.88	12.8
Root Cause Scoring	conj	0.66	0.80	0.86	0.77	12.6
	additive [†]	0.68	0.91	0.98	0.87	12.4

[†]Default configuration (zscore+max+additive). This table reports average time, *not* median.

Root Cause Scoring. We compare the additive score M_{add} (default) and conjunctive score M_{conj} (Equations 3–4). Table 5 shows both achieve strong performance. Additive scoring outperforms conjunctive scoring (68% vs. 66% Top-1, 91% vs. 80% Top-3). The additive score’s advantage emerges when internal anomalies are weak (violating the strong form of Assumption 2.4), where accumulating external evidence compensates for limited internal signal. The conjunctive score is more conservative but provably robust to arbitrary external amplification (Proposition 3.11).

Finding 7: Both scoring functions achieve comparable Top-1 accuracy (66–68%). Additive scoring shows higher Top-3/Top-5 accuracy (91% vs. 80% Top-3, 98% vs. 86% Top-5), particularly when internal anomalies are weak. Conjunctive scoring provides unconditional theoretical guarantees (Proposition 3.11).

Sensitivity to Data Length. After a failure is detected, it is critical to perform RCA rapidly, and execute proper resolving actions. *Can PRISM diagnose the root cause immediately upon failure detection, or must it wait for extended post-fault observations?* We vary the percentage of post-fault data from 10% to 100% (taking the first $k\%$ of post-fault observations temporally). Figure 4 reports results, compared with BARO, the second-best RCA baseline.

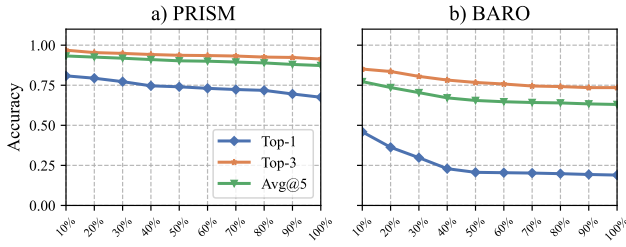


Figure 4. Sensitivity w.r.t. different post-fault data length.

PRISM achieves its highest accuracy with early observations, reaching 81% Top-1 at 10% data, then decreasing to 68% with full data. This pattern suggests that diagnosing immediately upon failure detection yields optimal results. The internal-external decomposition captures a diagnostic signal that emerges early. The root cause exhibits anomalies in *both* internal and external properties from the onset, while affected components show only external anomalies. This distinction, formalized in Lemma 3.12, is clearest before fault propagation accumulates noise in the observations.

BARO exhibits more severe degradation, with Top-1 accuracy decreasing from 46% at 10% data to 19% at full data. This occurs because fault propagation causes downstream components to accumulate increasingly severe symptoms over time. Eventually, downstream effects exhibit larger anomalies than the root cause (see Theorem C.3). PRISM is more resilient to this accumulation. While external anomalies grow in affected components, internal scores remain nominal per Axiom 2.6. The degradation in PRISM arises because accumulated noise affects the estimated anomaly scores, though the internal-external separation ensures PRISM degrades relatively slower than BARO.

Finding 8: PRISM achieves highest accuracy with early observations (81% Top-1 at 10% data), enabling immediate diagnosis. While both methods degrade with fault propagation, PRISM remains 3.6 \times more accurate than BARO at full data (68% vs. 19%).

4.5. Ablation Study

To answer RQ4, we ablate PRISM to verify that the internal-external decomposition is essential for effective RCA. We evaluate four variants: PRISM_{Marginal} ranks by highest marginal anomaly score, PRISM_{Internal} ranks by internal scores alone, PRISM_{External} ranks by external scores alone, and full PRISM. Table 6 presents the results.

PRISM_{Marginal} achieves only 19% Top-1 accuracy while full PRISM achieves 68%, a relative improvement of over 3 \times . As demonstrated in the case study (Table 4), the root cause is often *not* the component with the highest anomaly score. The internal-external decomposition enables PRISM to distinguish root causes from downstream effects.

PRISM_{Internal} achieves the lowest Top-1 accuracy at 15%. This confirms the limitation identified in Section 3.3, i.e.,

ranking by internal scores alone requires a strong form of Assumption 2.4 where faults manifest with sufficient magnitude in internal properties. In practice, this often fails. A code-level bug may not produce detectable spikes in resource metrics. When internal anomalies are weak, PRISM_{Internal} cannot reliably identify the root cause.

Table 6. Ablation Study over 735 Failure Cases

Method	Top-1	Top-3	Top-5	Avg @5	Time (ms)
PRISM _{Marginal}	0.19 (+)	0.74 (+)	0.85 (+)	0.63 (+)	10.6
PRISM _{Internal}	0.15 (+)	0.65 (+)	0.77 (+)	0.56 (+)	11.1
PRISM _{External}	0.54 (+)	0.81 (+)	0.89 (+)	0.77 (+)	11.9
PRISM	0.68	0.91	0.98	0.87	12.6

(+) Significantly outperforms ($p < 0.05$). This table reports average time, *not* median.

PRISM_{External} achieves 54% Top-1 accuracy, substantially better than internal-only, but still 21% worse than full PRISM. The limitation is fundamental. Fault propagation may cause affected components to exhibit high external anomalies (e.g., elevated latency due to upstream failures). As shown in Theorem C.3, downstream effects can exhibit larger anomalies than the root cause, making external scores alone insufficient to distinguish cause from effect.

Full PRISM achieves the best performance by leveraging *both* internal and external anomalies. This combination provides a discriminative criterion that the root cause exhibits anomalies in both property types, while affected components show only external anomalies (Lemma 3.12). This separation ensures that PRISM correctly rank the root cause above affected components, as proven in Theorem 3.13.

Finding 9: The internal-external decomposition is necessary for effective RCA. Internal scores alone fail when fault manifestation is weak. External scores alone fail due to fault propagation. PRISM combines both to achieve 68% Top-1, validating Theorem 3.13.

5. Conclusion

We addressed the question of how to find root causes when the dependency graph is unknown. While existing methods rank root cause candidates by marginal anomaly scores, we showed that they fail when downstream effects accumulate. We proposed PRISM, a simple yet principled RCA framework that requires evidence from both internal and external properties to distinguish root causes from downstream effects without constructing dependency graphs. We formalized the Component-Property Model and established theoretical guarantees for PRISM's correctness. We showed that deviation-based anomaly scorers satisfy conditions (monotonicity and injectivity) necessary for reliable RCA. Empirically, PRISM achieves 68% Top-1 accuracy on 735 failure cases across nine datasets, a 258% improvement over the best baseline. PRISM runs in 8 milliseconds per case, enabling real-time diagnosis in production systems.

Impact Statement

This paper presents work whose goal is to advance the field of Machine Learning. There are many potential societal consequences of our work, none which we feel must be specifically highlighted here.

References

Ahmed, T., Ghosh, S., Bansal, C., Zimmermann, T., Zhang, X., and Rajmohan, S. Recommending root-cause and mitigation steps for cloud incidents using large language models. In *2023 IEEE/ACM 45th International Conference on Software Engineering (ICSE)*, pp. 1737–1749. IEEE, 2023.

AWS. Building multi-tenant saas applications with aws lambda’s new tenant isolation mode. AWS Blogs, 2025a. <https://aws.amazon.com/blogs/compute/building-multi-tenant-saas-applications-with-aws-lambdas-new-tenant-isolation-mode/>.

AWS. What is soa (service-oriented architecture)? aws.amazon.com, 2025b. <https://aws.amazon.com/what-is/service-oriented-architecture/>.

Budhathoki, K., Minorics, L., Blöbaum, P., and Janzing, D. Causal structure-based root cause analysis of outliers. In *International conference on machine learning*, pp. 2357–2369. PMLR, 2022.

Chen, Y., Xie, H., Ma, M., Kang, Y., Gao, X., Shi, L., Cao, Y., Gao, X., Fan, H., Wen, M., et al. Automatic root cause analysis via large language models for cloud incidents. In *Proceedings of the Nineteenth European Conference on Computer Systems*, pp. 674–688, 2024a.

Chen, Y., Xie, H., Ma, M., Kang, Y., Gao, X., Shi, L., Cao, Y., Gao, X., Fan, H., Wen, M., et al. Automatic root cause analysis via large language models for cloud incidents. In *Proceedings of the Nineteenth European Conference on Computer Systems*, pp. 674–688, 2024b.

Chen, Y., Pan, J., Clark, J., Su, Y., Zheutlin, N., Bhavya, B., Arora, R. R., Deng, Y., Jha, S., and Xu, T. STRATUS: A multi-agent system for autonomous reliability engineering of modern clouds. In *The Thirty-ninth Annual Conference on Neural Information Processing Systems*, 2025. URL <https://openreview.net/forum?id=fYW1PKawwJ>.

Erl, T. *Service-oriented architecture: concepts, technology, and design*. Pearson Education India, 1900.

Erlang. Erlang/otp system documentation. Erlang Official Documentation, 2024. <https://www.erlang.org/doc/>.

Ferreira, M., Nicolet, V., Pham, L., Dodds, J., Kroening, D., Lynce, I., and Martins, R. Hypergraph-guided regex filter synthesis for event-based anomaly detection. *arXiv preprint arXiv:2509.06911*, 2025.

Google. Google - site reliability engineering, 2024. URL <https://sre.google/sre-book/monitoring-distributed-systems/>.

Gregg, B. Thinking methodically about performance. *Communications of the ACM*, 56(2):45–51, 2013.

Gregory, M. A. Optus triple zero outage has left multiple people dead. a telecommunications expert explains what went wrong – and how to fix it. *Law Society Journal*, Sep 22 2025. URL <https://lsj.com.au/articles/optus-triple-zero-outage-has-left-multiple-people-dead-a-telecommunications-expert-explains-what-went-wrong-and-how-to-fix-it/>. Accessed: 2025-12-22.

Han, X., Absar, S., Zhang, L., and Yuan, S. Root cause analysis of anomalies in multivariate time series through granger causal discovery. In *The Thirteenth International Conference on Learning Representations*, 2025. URL <https://openreview.net/forum?id=k38Th3x4d9>.

Hardt, M., Orchard, W. R., Blöbaum, P., Kirschbaum, E., and Kasiviswanathan, S. The petshop dataset—finding causes of performance issues across microservices. In *Causal Learning and Reasoning*, pp. 957–978. PMLR, 2024.

Ikram, A., Chakraborty, S., Mitra, S., Saini, S., Bagchi, S., and Kocaoglu, M. Root cause analysis of failures in microservices through causal discovery. *Advances in Neural Information Processing Systems*, 35:31158–31170, 2022.

Ikram, A., Lee, K., Agarwal, S., Saini, S. K., Bagchi, S., and Kocaoglu, M. Root cause analysis of failures from partial causal structures. In *The 41st Conference on Uncertainty in Artificial Intelligence*, 2025. URL <https://openreview.net/forum?id=5HeODZrG9E>.

Jha, S., Arora, R. R., Watanabe, Y., Yanagawa, T., Chen, Y., Clark, J., Bhavya, B., Verma, M., Kumar, H., Kitahara, H., et al. Itbench: Evaluating ai agents across diverse real-world it automation tasks. In *Forty-second International Conference on Machine Learning*, 2025. URL <https://openreview.net/forum?id=jP59rz1bZk>.

Kubernetes. Resource management for pods and containers. *Kubernetes Official Documentation*, 2024. <https://kubernetes.io/docs/concepts/configuration/manage-resources-containers/>.

Li, J., Chu, B. B., Scheller, I. F., Gagneur, J., and Maathuis, M. H. Root cause discovery via permutations and cholesky decomposition. *Journal of the Royal Statistical Society Series B: Statistical Methodology*, pp. qkaf066, 2025.

Li, M., Li, Z., Yin, K., Nie, X., Zhang, W., Sui, K., and Pei, D. Causal inference-based root cause analysis for online service systems with intervention recognition. In *Proceedings of the 28th ACM SIGKDD Conference on Knowledge Discovery and Data Mining*, pp. 3230–3240, 2022.

Lightbend. Akka: A guide to implementing the actor model. *Akka Official Documentation*, 2024. <https://doc.akka.io/>.

Lin, C.-M., Chang, C., Wang, W.-Y., Wang, K.-D., and Peng, W.-C. Root cause analysis in microservice using neural granger causal discovery. In *AAAI*, pp. 206–213, 2024. URL <https://doi.org/10.1609/aaai.v38i1.27772>.

Lin, J., Chen, P., and Zheng, Z. Microscope: Pinpoint performance issues with causal graphs in micro-service environments. In *International Conference on Service-Oriented Computing*, pp. 3–19. Springer, 2018.

McDonald, J. Wilcoxon signed-rank test. *Handbook of biological Statistics*, pp. 186–189, 2014.

Nagalapatti, L., Srivastava, A., Sarawagi, S., and Sharma, A. Robust root cause diagnosis using in-distribution interventions. In *The Thirteenth International Conference on Learning Representations*, 2025.

Orchard, W. R., Okati, N., Mejia, S. H. G., Blöbaum, P., and Janzing, D. Root cause analysis of outliers with missing structural knowledge. In *The Thirty-ninth Annual Conference on Neural Information Processing Systems*, 2025.

Pham, L., Ha, H., and Zhang, H. Baro: Robust root cause analysis for microservices via multivariate bayesian online change point detection. *Proceedings of the ACM on Software Engineering*, 1(FSE):2214–2237, 2024a.

Pham, L., Ha, H., and Zhang, H. Root cause analysis for microservice system based on causal inference: How far are we? In *Proceedings of the 39th IEEE/ACM International Conference on Automated Software Engineering*, pp. 706–715, 2024b.

Pham, L., Zhang, H., Ha, H., Salim, F., and Zhang, X. Rcae-val: A benchmark for root cause analysis of microservice systems with telemetry data. In *Companion Proceedings of the ACM on Web Conference 2025*, pp. 777–780, 2025.

Pham, L., Ha, H., Zhang, X., and Zhang, H. Torai: Multi-source root cause analysis for blind spots in microservice service call graph, 2026a.

Pham, L., Nicolet, V., Guan, H., Dodds, J., and Kroening, D. Eventadl: Open-box anomaly detection and localization framework for events in cloud-based service systems, 2026b.

Shan, H., Chen, Y., Liu, H., Zhang, Y., Xiao, X., He, X., Li, M., and Ding, W. ?-diagnosis: Unsupervised and real-time diagnosis of small-window long-tail latency in large-scale microservice platforms. In *The World Wide Web Conference*, pp. 3215–3222, 2019.

Wang, P., Xu, J., Ma, M., Lin, W., Pan, D., Wang, Y., and Chen, P. Cloudranger: Root cause identification for cloud native systems. In *IEEE/ACM International Symposium on Cluster, Cloud and Grid Computing*, pp. 492–502. IEEE, 2018.

Wang, Z., Liu, Z., Cheng, Y., Fan, Q., Li, S., Dang, Y., Zhang, P., Gao, Y., and Chen, E. Ragent: Cloud root cause analysis by autonomous agents with tool-augmented large language models. *arXiv preprint arXiv:2310.16340*, 2024.

Wilkie, T. The RED method: How to instrument your services. *Grafana Labs Blog*, 2018. <https://grafana.com/blog/the-red-method-how-to-instrument-your-services/>.

Wu, L., Tordsson, J., Elmroth, E., and Kao, O. Microrca: Root cause localization of performance issues in microservices. In *IEEE/IFIP Network Operations and Management Symposium*, pp. 1–9. IEEE, 2021.

Xin, R., Chen, P., and Zhao, Z. Causalrca: Causal inference based precise fine-grained root cause localization for microservice applications. *Journal of Systems and Software*, 203:111724, 2023.

Xu, J., Zhang, Q., Zhong, Z., He, S., Zhang, C., Lin, Q., Pei, D., He, P., Zhang, D., and Zhang, Q. OpenRCA: Can large language models locate the root cause of software failures? In *The Thirteenth International Conference on Learning Representations*, 2025. URL <https://openreview.net/forum?id=M4qNIzQYpd>.

Yahoo. Amazon’s One-Hour Downtime on Prime Day May Have Cost It \$72 Million to \$99 Million. <https://finance.yahoo.com/news/amazon-apos-one-hour-downtime-145350120.html>, Jul 2018. Accessed: 2025-12-23.

Zhang, L., Jia, T., Wang, K., Hong, W., Duan, C., He, M., and Li, Y. Adaptive root cause localization for microservice systems with multi-agent recursion-of-thought. *arXiv preprint arXiv:2508.20370*, 2025.

A. Proofs

Proof of Theorem 3.5 (Conditions Satisfied by Deviation-Based Scores). Let $S(x) = |x - c|/s$ with $s > 0$.

Monotonicity: If $|x - c| > |y - c|$, then dividing both sides by $s > 0$ preserves the inequality: $|x - c|/s > |y - c|/s$, hence $S(x) > S(y)$.

Injectivity: Follows directly from monotonicity by Lemma 3.4. \square

Proof of Theorem 3.6 (Injectivity is Necessary). Suppose $S(x_i) = S(x_j)$ for observations from distinct components $i \neq j$, despite $|x_i - c| \neq |x_j - c|$. Then no ranking criterion based solely on S can distinguish between components i and j . If the true root cause is component i (or j), any tie-breaking rule assigns rank 1 to the root cause with probability at most $1/2$ (assuming uniform random tie-breaking among tied components). More generally, if m components share the maximum score, RCA succeeds with probability at most $1/m$, violating the requirement that the root cause be ranked first. \square

Proof of Proposition 3.10 (Additive Score Validity). **Monotonicity.** For $M_{\text{add}}(s^I, s^E) = s^I + s^E - \log(1 + s^I + s^E)$, we have:

$$\frac{\partial M_{\text{add}}}{\partial s^I} = 1 - \frac{1}{1 + s^I + s^E} = \frac{s^I + s^E}{1 + s^I + s^E} \geq 0$$

with strict inequality when $s^I + s^E > 0$. By symmetry, $\frac{\partial M_{\text{add}}}{\partial s^E} \geq 0$ under the same condition. Thus M_{add} is monotonically non-decreasing in both arguments.

Internal boundedness. Assume bounded amplification: $s^E \leq \alpha s^I + \beta$ for constants $\alpha, \beta \geq 0$. Substituting and using $\log(1 + x) \geq 0$:

$$\begin{aligned} M_{\text{add}}(s^I, s^E) &= s^I + s^E - \log(1 + s^I + s^E) \\ &\leq s^I + (\alpha s^I + \beta) - \log(1 + (1 + \alpha)s^I + \beta) \\ &\leq (1 + \alpha)s^I + \beta \end{aligned}$$

Define $f(s) = (1 + \alpha)s + \beta$, which is monotonically increasing. When s^I is at nominal levels, $f(s^I)$ remains bounded by a small constant, ensuring affected components cannot achieve arbitrarily high scores regardless of external amplification. The root cause, with elevated s^I , achieves $M_{\text{add}} = \Theta(s^I)$, creating sufficient score separation for correct ranking (Theorem 3.13). \square

Proof of Proposition 3.11 (Conjunctive Score Validity). Monotonicity follows from the monotonicity of \min . Internal boundedness holds since $\min(s^I, s^E) \leq s^I$ for all s^I, s^E . \square

Proof of Lemma 3.12. **Part (1): Root cause has elevated internal score.** By definition, $S^I(C_r) = \phi(\{S(P) : P \in \mathbf{I}_r\})$. Since I_r^k is anomalous, $S(I_r^k) > 0$. For max and sum pooling, $\phi(X) \geq x$ for all $x \in X$ when elements are non-negative, hence $S^I(C_r) \geq S(I_r^k) > 0$. For mean pooling, the weaker bound $S^I(C_r) > 0$ holds.

Part (2): Affected components have nominal internal scores. By Axiom 2.6 (Inter-Component Isolation), there are no causal edges from any property of C_r to internal properties of C_a . Therefore, the fault in C_r cannot affect the internal properties of C_a , which remain drawn from the pre-fault distribution. Since anomaly scores are computed relative to this pre-fault distribution, $S^I(C_a)$ remains at nominal levels. Formally, let $\epsilon > 0$ be a threshold such that scores below ϵ are consistent with normal variation (e.g., the $(1 - \alpha)$ -quantile of the pre-fault score distribution). Then $S^I(C_a) \leq \epsilon$ with high probability.

Part (3): Score separation. By Assumption 2.4 (Diagnostic Sufficiency), the fault manifests as a detectable deviation. This means $S(I_r^k) > \epsilon$, i.e., the anomalous internal property exceeds the nominal threshold. Combined with Parts (1) and (2):

$$S^I(C_r) \geq S(I_r^k) > \epsilon \geq S^I(C_a)$$

Thus $S^I(C_r) > S^I(C_a)$ for any affected component C_a . \square

Remark A.1 (Sufficient Conditions for Theorem 3.13). To ensure $M(C_r) > M(C_a)$, the root cause must exhibit anomalies that exceed a nominal threshold ϵ in both internal and external properties. Formally, this requires $S^I(C_r) > \epsilon$ and $S^E(C_r) > \epsilon$, where ϵ is defined as the threshold above which anomaly scores are deemed “detectable” (e.g., the $(1 - \alpha)$ -quantile of the pre-fault score distribution). This interpretation is consistent with Assumption 2.4 (Diagnostic Sufficiency), which posits that the root cause exhibits detectable anomalies. The threshold ϵ makes this notion concrete. In practice, ϵ can be chosen using standard statistical methods (e.g., $\epsilon = 3$ for z-scores, or $\epsilon = 1.5 \times \text{IQR}$ for IQR-based scores).

Proof of Theorem 3.13 (PRISM Ranking Correctness). Let M be a scoring function satisfying monotonicity and internal boundedness (Definition 3.9) with bounding function f . Let C_r be the root cause and C_a be any affected component. Let $\epsilon > 0$ denote the nominal anomaly threshold. We proceed in three steps.

Step 1: Interpret “anomalies in both properties”. The hypothesis that the root cause exhibits “anomalies in both internal and external properties” means that its observed scores exceed the nominal threshold: $s_r^I = S^I(C_r) > \epsilon$ and $s_r^E = S^E(C_r) > \epsilon$. This is consistent with Assumption 2.4 (Diagnostic Sufficiency), which requires that faults manifest as detectable deviations. The threshold ϵ operationalizes this detectability requirement.

By Lemma 3.12(1), the root cause has $s_r^I \geq S(I_r^k) > 0$ for some anomalous internal property I_r^k . By Assumption 2.4, this manifestation exceeds the nominal threshold: $s_r^I > \epsilon$.

For the affected component C_a , by Axiom 2.6, faults in the root cause cannot directly affect internal properties of C_a . Hence by Lemma 3.12(2), $s_a^I = S^I(C_a) \leq \epsilon$ (the internal score remains at nominal levels). By Lemma 3.12(3), $s_r^I > s_a^I$.

Step 2: Bound the affected component’s score. By internal boundedness (Definition 3.9), there exists a monotonically increasing function $f : \mathbb{R}_{\geq 0} \rightarrow \mathbb{R}_{\geq 0}$ such that $M(s^I, s^E) \leq f(s^I)$ for all $s^I, s^E \geq 0$. For the affected component:

$$M(C_a) = M(s_a^I, s_a^E) \leq f(s_a^I) \leq f(\epsilon)$$

The second inequality follows from monotonicity of f and $s_a^I \leq \epsilon$.

Step 3: Establish ranking for both scorers.

Case 1 (Conjunctive Score): For $M_{\text{conj}}(s^I, s^E) = \min(s^I, s^E)$ with bounding function $f(s) = s$ (Proposition 3.11):

$$M_{\text{conj}}(C_r) = \min(s_r^I, s_r^E) > \min(\epsilon, \epsilon) = \epsilon$$

The inequality holds because both $s_r^I > \epsilon$ and $s_r^E > \epsilon$ by Step 1. Combined with Step 2, $M_{\text{conj}}(C_r) > \epsilon = f(\epsilon) \geq M_{\text{conj}}(C_a)$, yielding $M_{\text{conj}}(C_r) > M_{\text{conj}}(C_a)$.

Case 2 (Additive Score): For $M_{\text{add}}(s^I, s^E) = s^I + s^E - \log(1 + s^I + s^E)$, we compute:

$$M_{\text{add}}(C_r) = s_r^I + s_r^E - \log(1 + s_r^I + s_r^E)$$

Since $s_r^I > \epsilon$ and $s_r^E > \epsilon$, we have $s_r^I + s_r^E > 2\epsilon$. The logarithmic term satisfies $\log(1 + s_r^I + s_r^E) < s_r^I + s_r^E$ for all positive arguments (standard inequality). Under bounded external amplification (Proposition 3.10), the bounding function is $f(s) = (1 + \alpha)s + \beta$. Since $s_r^I > \epsilon$, we have:

$$M_{\text{add}}(C_r) \geq s_r^I > \epsilon \geq \frac{f(\epsilon)}{(1 + \alpha)} \text{ for } \alpha \geq 0$$

More directly, $M_{\text{add}}(C_r) = s_r^I + s_r^E - \log(1 + s_r^I + s_r^E) > s_r^I + \epsilon - \log(1 + s_r^I + \epsilon)$. When s_r^I is above the nominal level ϵ , this exceeds $f(\epsilon) = (1 + \alpha)\epsilon + \beta$. Thus $M_{\text{add}}(C_r) > f(\epsilon) \geq M_{\text{add}}(C_a)$, yielding $M_{\text{add}}(C_r) > M_{\text{add}}(C_a)$.

In both cases, $M(C_r) > M(C_a)$, as required. \square

Corollary A.2. Under the conditions of Theorem 3.13, for the conjunctive score $M_{\text{conj}} = \min(S^I, S^E)$:

$$M_{\text{conj}}(C_r) - M_{\text{conj}}(C_a) \geq \min(s_r^I, s_r^E) - \epsilon > 0$$

where $s_r^I = S^I(C_r)$ and $s_r^E = S^E(C_r)$. This provides a quantitative margin for correct ranking that grows with the severity of the root cause anomaly.

Proof. By Theorem 3.13, $M_{\text{conj}}(C_a) \leq s_a^I \leq \epsilon$. For the root cause, $M_{\text{conj}}(C_r) = \min(s_r^I, s_r^E)$. The margin follows directly:

$$M_{\text{conj}}(C_r) - M_{\text{conj}}(C_a) \geq \min(s_r^I, s_r^E) - \epsilon$$

As $s_r^I > \epsilon$, $s_r^E > \epsilon$ (hypothesis in Theorem 3.13), we have $\min(s_r^I, s_r^E) > \epsilon$, ensuring the margin is strictly positive. \square

Proof of Lemma 3.4 (Monotonicity implies Injectivity). Suppose $|x - c| \neq |y - c|$. Without loss of generality, assume $|x - c| > |y - c|$. By monotonicity, $S(x) > S(y)$, hence $S(x) \neq S(y)$. The converse fails: consider $S(x) = |x - c|$ for $x \geq c$ and $S(x) = 0$ for $x < c$; this is injective on $[c, \infty)$ but not monotonic globally. \square

Proof of Theorem C.1 (IT-Score Saturation). 1. The count $|\{i : \tau(x_i) \geq \tau(x)\}|$ takes values in $\{0, 1, \dots, k\}$. The minimum positive count is 1, giving maximum score $-\log(1/k) = \log k$.

2. When $\tau(x) > \max_{i \in [k]} \tau(x_i)$, no reference observation has τ -value at least as large as $\tau(x)$, so the count is 0. With Laplace smoothing (replacing 0 with 0.5 and k with $k + 0.5$), we obtain:

$$\hat{S}_{\text{IT}}(x) = -\log \frac{0.5}{k + 0.5} \approx \log(2k) \quad (6)$$

3. All observations exceeding the reference maximum yield count 0 (or 0.5 with smoothing). Hence, they receive identical IT-scores regardless of their actual τ values: whether $\tau(x^{(1)}) = 10$ or $\tau(x^{(2)}) = 1000$, both receive $\hat{S}_{\text{IT}} = \log(2k)$. \square

Proof of Theorem C.3 (Counterexample to Marginal Score Ordering). Consider a caller-callee system with:

- ▷ C_{callee} (root cause): internal fault causes latency $L_{\text{callee}} = L_0 + \Delta$
- ▷ C_{caller} : makes k sequential calls to callee, observing latency $L_{\text{caller}} = k \cdot L_{\text{callee}} = k(L_0 + \Delta)$

The external anomaly scores satisfy:

$$S^E(C_{\text{caller}}) = S(k(L_0 + \Delta)) > S(L_0 + \Delta) = S^E(C_{\text{callee}})$$

for $k > 1$, since IT scores are monotonic in the feature value.

However, the internal scores satisfy:

$$S^I(C_{\text{callee}}) \text{ is high} \quad (\text{root cause has internal anomaly})$$

$$S^I(C_{\text{caller}}) \text{ is low} \quad (\text{caller's internal properties are normal})$$

Thus, marginal score ordering (as in Orchard et al. (2025)'s Score Ordering) would incorrectly identify C_{caller} as the root cause. PRISM correctly identifies C_{callee} because:

$$M_{\text{conj}}(C_{\text{callee}}) = \min(\text{high}, \text{high}) > \min(\text{low}, \text{high}) = M_{\text{conj}}(C_{\text{caller}})$$

\square

Proof of Corollary C.4 (Deviation-Based Scores Enable RCA). By Theorem 3.5, deviation-based scores are injective almost surely under continuous distributions. Combined with monotonicity, the component with the largest deviation receives the highest score and is ranked first. \square

Proof of Corollary C.5 (IT-Scores Fail for RCA Under Saturation). By Theorem C.1 and Corollary C.2, all components with τ -values exceeding the reference maximum receive identical IT-scores. By Theorem 3.6, non-injectivity implies RCA failure. \square

B. Related Work

Causal Graph-Based RCA. A prevalent approach to RCA constructs causal or dependency graphs from observational data and traverses them to identify root causes. Microscope (Lin et al., 2018) constructs service causal graphs by analyzing metrics time series data. CloudRanger (Wang et al., 2018) uses Pearson correlation to build dependency graphs and employs second-order random walks for root cause localization. MicroRCA (Wu et al., 2021) constructs attributed graphs from metrics and traces. CausalRCA (Xin et al., 2023) applies DAG-GNN to learn causal structures and uses PageRank for ranking. More recent work has explored alternative graph construction strategies. Ikram et al. (2022) propose a hierarchical approach that treats failures as interventions to reduce the number of conditional independence tests. CIRCA (Li et al., 2022) formulates RCA as intervention recognition in a Causal Bayesian Network constructed from call graphs. RUN (Lin et al., 2024) employs neural Granger causal discovery with contrastive learning to capture temporal dependencies that PC-based methods miss. AERCA (Han et al., 2025) integrates Granger causal discovery with anomaly detection for multivariate time series. EventADL (Pham et al., 2026b) constructs an intervention graph from events data and performs time-aware random walk over the constructed graph to localize the root cause interventions from given detected anomalies (Ferreira et al., 2025). These methods share a common pipeline: construct a causal graph using causal discovery methods or correlation-based approaches, then traverse or score nodes to identify root causes. However, as highlighted by Pham et al. (2024b), these graph-based methods are often inefficient and ineffective. As shown in Section 4.2, PC-PageRank achieves only 9% Top-1 accuracy on the RCAEval benchmark. PRISM bypasses graph construction entirely, achieving 68% Top-1 accuracy while running 150 \times faster.

Anomaly Score-Based RCA. An alternative approach ranks root cause candidates directly by anomaly scores without constructing causal graphs. Budhathoki et al. (2022) formalize RCA as quantifying each variable’s contribution to an outlier score using Shapley values, requiring a known causal graph and structural causal model. Orchard et al. (2025) propose IT-based anomaly scoring with traversal methods that operate without structural knowledge, assuming the root cause exhibits the highest anomaly score. Li et al. (2025) exploit permutation invariance in linear SCMs to identify root causes via Cholesky decomposition. BARO (Pham et al., 2024a) combines Bayesian online change point detection with IQR-based scoring for robust anomaly quantification. TORAI (Pham et al., 2026a) computes the anomaly severity of each components, then cluster them into normal and abnormal groups for further causal inference-based RCA. Nagalapatti et al. (2025) propose In-Distribution Interventions (IDI), which identifies root causes by testing both anomaly and fix conditions using interventional rather than counterfactual estimates, improving robustness when anomalies fall outside training distributions. From a theoretical perspective, Ikram et al. (2025) establish a connection between RCA and Interactive Graph Search, proving that any algorithm relying solely on marginal invariance tests requires at least $\Omega(\log n)$ tests. A common assumption across these methods is that the root cause exhibits the *highest* anomaly score among all candidates. However, as we prove in Theorem C.3, this assumption fails when downstream effects accumulate, for example, when a callee is invoked multiple times, its small delay can amplify into a much larger delay at the caller. PRISM addresses this limitation by leveraging *both* internal and external anomalies, distinguishing root causes from propagated effects even when external anomalies are amplified.

LLM-Based RCA. Recent work explores large language models (LLMs) for RCA, particularly in cloud environments. RCLAgent (Zhang et al., 2025), which we use as a baseline, employs multi-agent recursion-of-thought to iteratively localize root causes using topology graphs and call graph information. Similarly, Stratus (Chen et al., 2025) proposes a multi-agent system for autonomous reliability engineering in modern clouds. At the industry scale, RCAgent (Wang et al., 2024) is a tool-augmented LLM agent deployed at Alibaba Cloud that autonomously gathers evidence and reasons about root causes. Microsoft has deployed multiple LLM-based solutions. RCACopilot (Chen et al., 2024b) uses GPT-4 with retrieval-augmented generation for automated incident diagnosis, while Ahmed et al. (2023) focus on recommending both root causes and mitigation steps for Azure incidents. Chen et al. (2024a) further demonstrate LLM effectiveness for cloud incident diagnosis through automated reasoning pipelines. The OpenRCA benchmark (Xu et al., 2025) provides a systematic evaluation framework with 335 failures and 68GB of telemetry data from enterprise systems, revealing that even with a specialized RCA-agent, Claude 3.5 solves only 11.34% of failure cases. While these methods leverage rich contextual information from logs, traces, and documentation, they incur substantial latency. RCLAgent requires 79 seconds per failure case compared to PRISM’s 8 milliseconds, a 9,700 \times difference. Furthermore, their effectiveness depends on call graphs and heterogeneous data sources that may not always be available in production systems. PRISM provides a lightweight alternative that operates solely on metrics data with theoretical guarantees.

C. Additional Results

C.1. Effectiveness of PRISM

This section presents detailed per-dataset results complementing the aggregate analysis in Section 4.2. The following tables report performance across all fault types for each of the nine datasets in the RCAEval benchmark.

C.1.1. ONLINE BOUTIQUE (UNIMODAL)

On RE1OB (Online Boutique), PRISM achieves 61% Top-1 and 92% Top-3 accuracy. Performance is strongest on resource faults, with MEM reaching 84% Top-1 and DELAY reaching 76% Top-1, where internal properties directly reflect the injected fault. Network faults prove more challenging. LOSS achieves only 28% Top-1, as packet loss may not immediately manifest in internal resource metrics.

Table 7. RCA method performance on RE1OB (Online Boutique with unimodal data).

Method	CPU			DELAY			DISK			LOSS			MEM			AVERAGE			STAT
	Top-1	Top-3	Avg@5																
Smooth-Traversal	0.04	0.25	0.19	0.08	0.20	0.16	0.04	0.08	0.07	0.04	0.17	0.13	0.08	0.16	0.13	0.06	0.17	0.14	$7.3e^{-20}_{(+)}$
Simple-Traversal	0.08	0.12	0.11	0.08	0.24	0.22	0.04	0.20	0.16	0.08	0.17	0.16	0.08	0.16	0.13	0.07	0.18	0.16	$9.4e^{-20}_{(+)}$
Counterfactual	0.04	0.12	0.13	0.08	0.28	0.27	0.20	0.24	0.30	0.12	0.25	0.27	0.08	0.16	0.20	0.11	0.21	0.23	$5.3e^{-19}_{(+)}$
Cholesky	0.08	0.20	0.22	0.08	0.24	0.22	0.12	0.28	0.28	<u>0.16</u>	0.32	0.34	0.12	0.16	0.24	0.11	0.24	0.26	$2.6e^{-18}_{(+)}$
PC-PageRank	0.00	0.12	0.13	0.08	0.16	0.19	0.16	0.44	0.42	0.04	0.36	0.31	0.08	0.24	0.26	0.07	0.26	0.26	$6.0e^{-19}_{(+)}$
Score-Ordering	0.08	0.42	0.34	0.12	0.32	0.33	0.12	0.32	0.36	0.08	0.29	0.37	0.08	0.24	0.27	0.10	0.32	0.33	$3.7e^{-18}_{(+)}$
BARO	<u>0.12</u>	<u>0.75</u>	<u>0.60</u>	<u>0.24</u>	<u>0.84</u>	<u>0.73</u>	<u>0.36</u>	<u>0.96</u>	<u>0.81</u>	0.04	<u>0.48</u>	<u>0.43</u>	<u>0.32</u>	<u>0.96</u>	<u>0.82</u>	<u>0.22</u>	<u>0.80</u>	<u>0.68</u>	$4.1e^{-13}_{(+)}$
PRISM	0.52	0.92	0.85	0.76	1.00	0.95	0.64	1.00	0.92	0.28	0.68	0.66	0.84	1.00	0.96	0.61	0.92	0.87	N/A

C.1.2. SOCK SHOP (UNIMODAL)

On RE1SS (Sock Shop), PRISM demonstrates strong performance with 75% Top-1 and 97% Top-3 accuracy. The method achieves 84% Top-1 on CPU faults and 80% Top-1 on DELAY, DISK, and MEM faults. All improvements over baselines are statistically significant ($p < 0.05$).

Table 8. RCA method performance on RE1SS (Sock Shop with unimodal data).

Method	CPU			DELAY			DISK			LOSS			MEM			AVERAGE			STAT
	Top-1	Top-3	Avg@5																
Counterfactual	0.16	0.24	0.22	0.08	0.12	0.12	0.16	0.24	0.21	0.04	0.04	0.04	0.16	0.16	0.18	0.12	0.16	0.15	$7.8e^{-21}_{(+)}$
Smooth-Traversal	0.12	0.24	0.22	0.00	0.24	0.22	0.04	0.16	0.14	0.00	0.16	0.11	0.04	0.20	0.17	0.04	0.20	0.17	$6.9e^{-21}_{(+)}$
PC-PageRank	0.20	0.24	0.27	0.20	0.28	0.25	0.20	0.40	0.32	0.24	0.44	0.39	0.04	0.24	0.18	0.18	0.32	0.28	$1.1e^{-18}_{(+)}$
Cholesky	0.08	0.20	0.23	0.08	0.20	0.21	0.04	0.32	0.34	0.12	0.36	0.40	0.12	0.40	0.37	0.09	0.30	0.31	$1.1e^{-18}_{(+)}$
Simple-Traversal	0.16	0.32	0.32	0.08	0.32	0.30	0.08	0.36	0.35	0.12	0.32	0.31	0.12	0.28	0.27	0.11	0.32	0.31	$1.1e^{-18}_{(+)}$
Score-Ordering	0.16	<u>0.40</u>	0.36	0.20	0.48	0.42	0.04	0.36	0.38	0.12	0.32	0.35	0.16	0.32	0.34	0.14	0.38	0.37	$3.0e^{-18}_{(+)}$
BARO	<u>0.40</u>	1.00	<u>0.86</u>	<u>0.60</u>	<u>0.92</u>	<u>0.84</u>	<u>0.40</u>	<u>0.96</u>	<u>0.84</u>	<u>0.28</u>	<u>0.76</u>	<u>0.70</u>	<u>0.56</u>	<u>0.92</u>	<u>0.86</u>	<u>0.45</u>	<u>0.91</u>	<u>0.82</u>	$3.2e^{-6}_{(+)}$
PRISM	0.84	1.00	0.96	0.80	0.96	0.93	0.80	1.00	0.95	0.52	0.92	0.83	0.80	0.96	0.93	0.75	0.97	0.92	N/A

C.1.3. TRAIN TICKET (UNIMODAL)

On RE1TT (Train Ticket), the most complex system with 64 components, PRISM achieves 33% Top-1 and 71% Top-3 accuracy while all baselines remain below 10% Top-1. The method achieves 68% Top-1 on MEM faults and 36% on CPU. The increased system complexity poses challenges for all methods, yet PRISM maintains substantial improvements.

Table 9. RCA method performance on RE1TT (Train Ticket with unimodal data).

Method	CPU			DELAY			DISK			LOSS			MEM			AVERAGE			STAT
	Top-1	Top-3	Avg@5																
PC-PageRank	0.00	0.00	0.00	0.00	0.00	0.00	0.00	0.00	0.00	0.00	0.00	0.00	0.00	0.00	0.02	0.00	0.00	0.00	$1.2e^{-19}_{(+)}$
Counterfactual	0.00	0.08	0.08	0.00	0.04	0.02	0.00	0.04	0.03	<u>0.00</u>	0.00	0.00	0.00	0.04	0.02	0.00	0.04	0.03	$3.6e^{-19}_{(+)}$
Simple-Traversal	0.00	0.04	0.06	0.00	0.04	0.02	0.00	0.00	0.01	<u>0.00</u>	0.00	0.03	0.00	0.04	0.02	0.00	0.02	0.03	$3.6e^{-19}_{(+)}$
Smooth-Traversal	0.00	0.00	0.01	<u>0.04</u>	0.08	0.06	0.00	0.04	0.03	<u>0.00</u>	0.04	0.03	0.00	0.00	0.02	0.01	0.03	0.03	$4.3e^{-19}_{(+)}$
Cholesky	0.04	0.12	0.12	0.00	0.00	0.00	0.00	0.00	0.05	<u>0.00</u>	0.04	0.05	0.00	0.00	0.02	0.01	0.03	0.05	$3.6e^{-19}_{(+)}$
Score-Ordering	0.00	0.04	0.04	<u>0.04</u>	0.04	0.07	<u>0.04</u>	0.04	<u>0.09</u>	<u>0.00</u>	<u>0.08</u>	0.06	0.04	0.08	0.08	0.02	0.06	0.07	$4.3e^{-19}_{(+)}$
BARO	<u>0.12</u>	<u>0.52</u>	<u>0.42</u>	<u>0.04</u>	<u>0.24</u>	<u>0.24</u>	0.00	<u>0.08</u>	0.06	<u>0.00</u>	<u>0.08</u>	<u>0.11</u>	0.28	<u>0.68</u>	<u>0.58</u>	<u>0.09</u>	<u>0.32</u>	<u>0.28</u>	$1.3e^{-16}_{(+)}$
PRISM	0.36	0.80	0.73	0.24	0.68	0.61	0.12	0.64	0.59	0.24	0.52	0.54	0.68	0.92	0.89	0.33	0.71	0.67	N/A

C.1.4. SOCK SHOP (MULTIMODAL)

On RE2SS (Sock Shop with multimodal data), PRISM achieves 86% Top-1 and 96% Top-3 accuracy. Perfect accuracy is observed on MEM faults (100% Top-1), with strong performance on CPU (87%), DISK (93%), and LOSS (80%) faults. The multimodal data provides richer internal-external signal separation.

Table 10. RCA method performance on RE2SS (Sock Shop with multimodal data).

Method	CPU			DELAY			DISK			LOSS			MEM			SOCKET			AVERAGE			STAT			
	Top-1	Top-3	Avg@5																						
Counterfactual	0.13	0.13	0.13	0.00	0.07	0.04	0.13	0.27	0.24	0.27	0.27	0.29	0.07	0.07	0.07	0.07	0.07	0.07	0.12	0.11	0.14	0.15	$1.3e^{-15}_{(+)}$		
Smooth-Traverser	0.20	0.27	0.24	0.00	0.13	0.08	0.00	0.27	0.21	0.00	0.20	0.12	0.13	0.27	0.21	0.13	0.27	0.24	0.33	0.40	0.41	0.17	0.30	0.27	$2.5e^{-15}_{(+)}$
PC-PageRank	0.20	0.33	0.29	0.07	0.33	0.27	0.13	0.20	0.20	0.13	0.27	0.21	0.13	0.27	0.24	0.33	0.40	0.41	0.17	0.30	0.27	0.20	0.30	0.27	$2.5e^{-14}_{(+)}$
Cholesky	0.07	0.27	0.27	0.07	0.13	0.20	0.20	0.53	0.40	0.07	0.40	0.35	0.00	0.07	0.06	0.16	0.07	0.40	0.33	0.08	0.30	0.28	0.27	$1.3e^{-14}_{(+)}$	
Simple-Traverser	0.27	0.40	0.37	0.07	0.47	0.40	0.07	0.60	0.44	0.00	0.40	0.25	0.20	0.40	0.35	0.20	0.33	0.31	0.13	0.43	0.35	0.27	0.35	0.35	$1.8e^{-13}_{(+)}$
Score-Ordering	0.20	0.40	0.41	0.07	0.40	0.37	0.13	0.47	0.43	0.13	0.53	0.45	0.13	0.40	0.36	0.13	0.53	0.49	0.13	0.46	0.42	0.27	0.42	0.42	$7.5e^{-13}_{(+)}$
BARO	0.00	0.73	0.60	0.00	0.67	0.57	0.67	0.93	0.85	0.07	0.93	0.71	0.13	1.00	0.79	0.00	0.60	0.51	0.14	0.81	0.67	0.27	0.67	0.67	$8.1e^{-14}_{(+)}$
PRISM	0.87	1.00	0.97	0.73	0.93	0.89	0.93	0.93	0.93	0.80	1.00	0.96	1.00	1.00	1.00	0.80	0.87	0.91	0.86	0.96	0.94	N/A			

C.1.5. TRAIN TICKET (MULTIMODAL)

On RE2TT (Train Ticket with multimodal data), PRISM achieves 51% Top-1 and 89% Top-3 accuracy. Most baselines fail entirely on this complex system (0% Top-1), while PRISM achieves 73% Top-1 on DISK faults and 67% on MEM. Only BARO shows partial competitiveness (32% Top-1).

Table 11. RCA method performance on RE2TT (Train Ticket with multimodal data).

Method	CPU			DELAY			DISK			LOSS			MEM			SOCKET			AVERAGE			STAT
	Top-1	Top-3	Avg@5																			
PC-PageRank	0.00	0.00	0.00	0.00	0.00	0.00	0.00	0.00	0.00	0.00	0.00	0.00	0.00	0.00	0.00	0.00	0.00	0.00	0.00	0.00	0.00	$4.9e^{-15}_{(+)}$
RCLAgent	0.00	0.00	0.00	0.00	0.00	0.00	0.00	0.00	0.00	0.00	0.00	0.00	0.00	0.00	0.00	0.00	0.00	0.00	0.00	0.00	0.00	$4.0e^{-15}_{(+)}$
Counterfactual	0.00	0.00	0.00	0.00	0.00	0.00	0.00	0.07	0.07	0.00	0.00	0.01	0.00	0.07	0.05	0.00	0.00	0.00	0.02	0.02	0.02	$4.9e^{-15}_{(+)}$
Simple-Traverser	0.00	0.00	0.03	0.00	0.00	0.01	0.07	0.07	0.07	0.00	0.00	0.03	0.00	0.00	0.00	0.00	0.00	0.00	0.01	0.01	0.02	$4.9e^{-15}_{(+)}$
Cholesky	0.00	0.13	0.08	0.00	0.00	0.00	0.00	0.00	0.00	0.07	0.07	0.07	0.00	0.00	0.01	0.00	0.07	0.05	0.01	0.04	0.04	$1.4e^{-14}_{(+)}$
Smooth-Traverser	0.07	0.07	0.09	0.00	0.00	0.00	0.00	0.07	0.05	0.00	0.07	0.04	0.07	0.13	0.11	0.00	0.00	0.00	0.02	0.06	0.05	$5.3e^{-15}_{(+)}$
Score-Ordering	0.07	0.07	0.13	0.00	0.00	0.03	0.07	0.13	0.12	0.00	0.07	0.09	0.07	0.07	0.07	0.00	0.00	0.00	0.03	0.06	0.07	$2.9e^{-14}_{(+)}$
BARO	0.20	0.73	0.65	0.00	0.20	0.19	0.73	1.00	0.95	0.00	0.20	0.19	0.60	1.00	0.92	0.40	0.47	0.52	0.32	0.60	0.57	$1.5e^{-5}_{(+)}$
PRISM	0.47	0.87	0.80	0.47	0.87	0.79	0.73	1.00	0.95	0.20	0.67	0.52	0.67	0.93	0.88	0.53	1.00	0.88	0.51	0.89	0.80	N/A

C.1.6. ONLINE BOUTIQUE (CODE-LEVEL FAULTS)

On RE3OB (Online Boutique with code-level faults), PRISM achieves 90% Top-1 and 98% Top-3 accuracy. Performance is highest on F2, F3, and F4 faults (100% Top-1), with strong performance on F5 (83% Top-1). F1 achieves 67% Top-1.

Table 12. RCA method performance on RE3OB (Online Boutique with code-level faults).

Method	F1			F2			F3			F4			F5			AVERAGE			STAT
	Top-1	Top-3	Avg@5																
Smooth-Traverser	0.11	0.11	0.11	0.00	0.33	0.27	0.00	0.17	0.13	0.17	0.17	0.17	0.00	0.17	0.13	0.06	0.19	0.16	$8.8e^{-6}_{(+)}$
Counterfactual	0.11	0.11	0.11	0.33	0.33	0.47	0.00	0.17	0.13	0.00	0.17	0.13	0.00	0.00	0.09	0.16	0.17	$8.8e^{-6}_{(+)}$	
Cholesky	0.11	0.33	0.27	0.00	0.33	0.20	0.33	0.50	0.43	0.00	0.00	0.10	0.33	0.33	0.37	0.16	0.30	0.27	$3.7e^{-5}_{(+)}$
RCLAgent	0.25	0.25	0.25	0.00	0.00	0.00	0.17	0.33	0.30	0.33	0.50	0.47	0.17	0.50	0.40	0.18	0.32	0.28	$3.7e^{-5}_{(+)}$
PC-PageRank	0.11	0.22	0.33	0.00	0.00	0.27	0.00	0.17	0.13	0.00	0.33	0.27	0.33	0.50	0.57	0.09	0.24	0.31	$3.7e^{-5}_{(+)}$
Simple-Traverser	0.11	0.22	0.20	0.33	0.67	0.60	0.17	0.50	0.43	0.17	0.33	0.30	0.17	0.33	0.30	0.19	0.41	0.37	$3.7e^{-5}_{(+)}$
Score-Ordering	0.22	0.44	0.44	0.33	0.67	0.67	0.17	0.67	0.50	0.17	0.17	0.30	0.17	0.50	0.43	0.21	0.49	0.47	$4.7e^{-5}_{(+)}$
BARO	0.00	1.00	0.80	0.00	1.00	0.73	0.17	1.00	0.83	0.00	1.00	0.77	0.00	0.50	0.40	0.03	0.90	0.71	$2.5e^{-4}_{(+)}$
PRISM	0.67	0.89	0.87	1.00	0.83	1.00	0.97	0.90	0.98	0.97	N/A								

C.1.7. SOCK SHOP (CODE-LEVEL FAULTS)

On RE3SS (Sock Shop with code-level faults), PRISM achieves 20% Top-1 and 79% Top-3 accuracy. The high Top-3 relative to Top-1 indicates the root cause consistently appears among top candidates, with the highest performance on F1 (60% Top-1).

C.1.8. TRAIN TICKET (CODE-LEVEL FAULTS)

On RE3TT (Train Ticket with code-level faults), PRISM achieves 90% Top-1 and perfect 100% Top-3 accuracy. Perfect accuracy is observed on F1, F2, and F4 faults (100% Top-1), with F3 achieving 60% Top-1. All baselines fail substantially,

Table 13. RCA method performance on RE3SS (Sock Shop with code-level faults).

Method	F1			F2			F3			F4			AVERAGE			STAT
	Top-1	Top-3	Avg@5													
Counterfactual	0.10	0.30	0.30	<u>0.00</u>	0.00	0.07	<u>0.10</u>	0.10	0.14	0.14	0.43	0.34	0.09	0.21	0.21	$7.9e^{-4}_{(+)}$
PC-PageRank	<u>0.20</u>	0.40	0.42	<u>0.00</u>	<u>0.33</u>	0.27	0.00	0.20	0.18	0.29	0.57	0.57	0.12	0.38	0.36	0.008 ₍₊₎
Cholesky	<u>0.20</u>	0.50	0.44	<u>0.00</u>	<u>0.33</u>	0.27	0.20	0.40	0.44	0.14	0.43	0.43	0.14	0.42	0.39	0.016 ₍₊₎
Score-Ordering	0.10	0.40	0.36	<u>0.00</u>	0.00	0.07	<u>0.10</u>	<u>0.50</u>	0.42	0.57	0.86	0.77	<u>0.19</u>	0.44	0.40	0.063 _(≈)
Simple-Traversal	0.10	0.50	0.36	<u>0.00</u>	<u>0.33</u>	0.27	0.20	0.40	0.40	<u>0.43</u>	<u>0.71</u>	<u>0.69</u>	0.18	0.49	0.43	0.063 _(≈)
BARO	<u>0.20</u>	<u>0.70</u>	<u>0.62</u>	<u>0.00</u>	<u>0.33</u>	0.40	0.20	0.40	0.44	0.29	0.57	0.60	0.17	0.50	0.52	0.063 _(≈)
Smooth-Traversal	0.10	<u>0.70</u>	0.52	0.33	1.00	0.80	<u>0.10</u>	<u>0.50</u>	<u>0.48</u>	0.29	0.43	0.40	0.20	<u>0.66</u>	<u>0.55</u>	0.063 _(≈)
PRISM	0.60	1.00	0.88	0.00	1.00	0.73	0.20	0.60	0.60	0.00	0.57	0.51	0.20	0.79	0.68	N/A

with even the second-best method (BARO) achieving only 20% Top-1 despite 100% Top-3. This demonstrates PRISM’s robustness on complex systems where other methods cannot reliably identify the root cause.

Table 14. RCA method performance on RE3TT (Train Ticket with code-level faults).

Method	F1			F2			F3			F4			AVERAGE			STAT
	Top-1	Top-3	Avg@5													
PC-PageRank	0.00	0.00	0.00	0.00	0.00	0.00	0.00	0.00	0.00	0.00	0.00	0.00	0.00	0.00	0.00	$1.6e^{-6}_{(+)}$
RCLAgent	0.00	0.00	0.00	0.00	0.00	0.00	0.00	0.00	0.00	0.00	0.00	0.00	0.00	0.00	0.00	$1.6e^{-6}_{(+)}$
Smooth-Traversal	0.00	0.00	0.00	0.00	0.00	0.00	0.00	0.00	0.04	0.00	<u>0.00</u>	0.00	0.00	0.00	0.01	$1.6e^{-6}_{(+)}$
Cholesky	0.00	<u>0.14</u>	0.11	0.00	0.00	0.00	0.00	0.00	0.00	0.00	<u>0.00</u>	0.00	0.00	0.04	0.03	$1.6e^{-6}_{(+)}$
Counterfactual	0.00	0.00	0.00	<u>0.14</u>	<u>0.14</u>	0.14	0.00	0.00	0.00	0.00	<u>0.00</u>	0.00	0.04	0.04	0.04	$1.6e^{-6}_{(+)}$
Score-Ordering	0.00	0.00	0.00	0.00	<u>0.14</u>	0.11	0.10	<u>0.10</u>	0.14	0.00	<u>0.00</u>	0.00	0.03	0.06	0.06	$1.6e^{-6}_{(+)}$
Simple-Traversal	0.00	<u>0.14</u>	0.09	0.00	<u>0.14</u>	0.17	0.00	<u>0.10</u>	0.08	0.00	<u>0.00</u>	0.00	0.00	<u>0.10</u>	0.08	$1.6e^{-6}_{(+)}$
BARO	<u>0.14</u>	1.00	<u>0.83</u>	<u>0.14</u>	1.00	<u>0.74</u>	0.20	1.00	<u>0.80</u>	<u>0.33</u>	1.00	<u>0.87</u>	<u>0.20</u>	1.00	<u>0.81</u>	$2.9e^{-4}_{(+)}$
PRISM	1.00	1.00	1.00	1.00	1.00	1.00	0.60	1.00	0.90	1.00	1.00	1.00	0.90	1.00	0.97	N/A

C.2. Case study: IT-Score Saturation Problem

Orchard et al. (2025) propose using IT (Information-Theoretic) anomaly scores for root cause analysis. Given k pre-fault observations, the IT-score is estimated as:

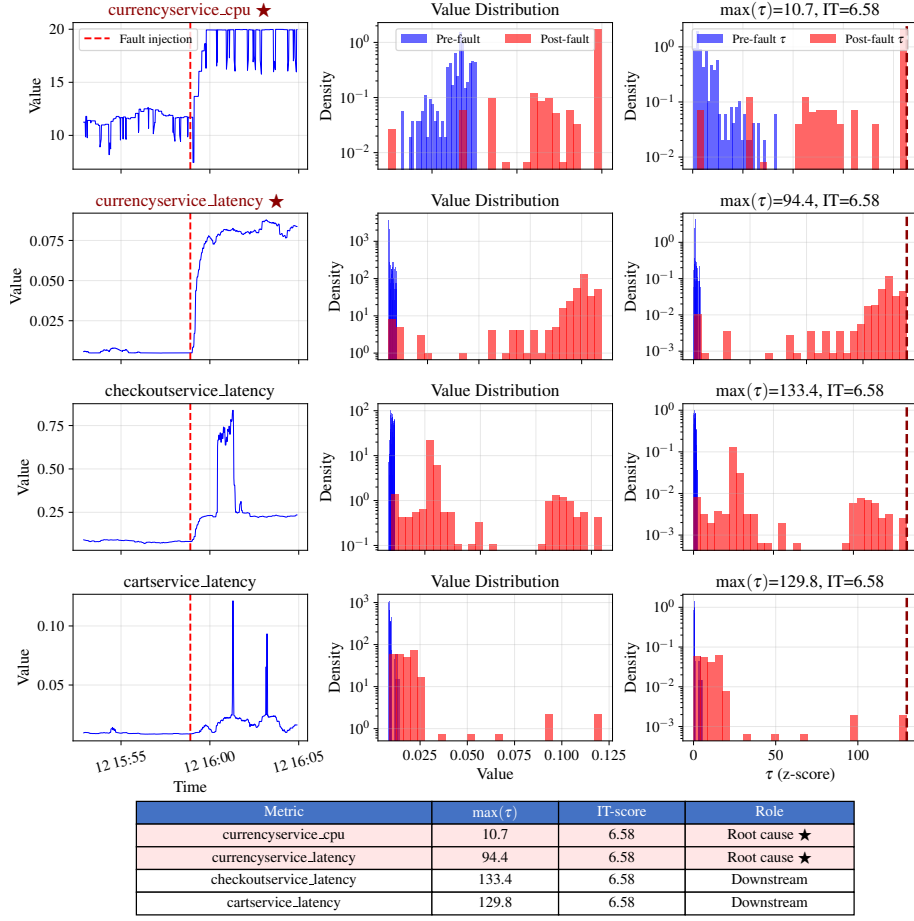
$$\hat{S}(x) = -\log \frac{|\{i : \tau(x_i) \geq \tau(x)\}|}{k} \quad (7)$$

where τ is a feature function (e.g., z-score or IQR-based score).

However, this formulation suffers from a *saturation problem* in practice. When a failure occurs, multiple components exhibit anomalies that exceed their normal variation. If the maximum post-fault τ -score exceeds *all* pre-fault τ -scores, the count in Eq. 7 becomes zero, yielding identical IT-scores for all affected components.

Figure 5 demonstrates this phenomenon on a real failure case from the Online Boutique benchmark. A disk fault was injected into `currencyService`, causing anomalies in both root cause metrics (`currencyService.cpu`, `currencyService.latency`) and downstream latency metrics (`checkoutService.latency`, `cartService.latency`). Despite max τ values ranging from 10.7 to 133.4 (a 12 \times difference), all metrics receive identical IT-scores of approximately 6.58. This occurs because with $k = 360$ pre-fault samples, the maximum possible IT-score is $-\log(1/360) \approx 5.89$, and all metrics with post-fault anomalies exceeding historical bounds saturate near this ceiling.

The fundamental limitation is that IT-scores measure *whether* an anomaly occurred (a binary notion of “surprise”), not *how severe* it is relative to other anomalies. This renders IT-scores ineffective for ranking candidate root causes in systems where failures propagate to multiple downstream components.



Despite $12 \times$ difference in $\max(\tau)$, all metrics receive identical IT-scores (saturated at $\log(2k) \approx 6.58$)

Figure 5. IT-score saturation on a disk fault in `currencyService`. Despite vastly different anomaly magnitudes (max τ ranging from 10.7 to 133.4), all metrics receive identical IT-scores of approximately 6.58. The root cause metrics (`currencyService.cpu` and `currencyService.latency`, marked \star) cannot be distinguished from downstream effects (`checkoutService.latency`, `cartService.latency`) based on IT-scores alone. The summary table quantifies the saturation: a $12 \times$ difference in τ magnitude yields identical scores.

C.3. IT-Score Saturation Theory

The Information-Theoretic (IT) score transforms deviation through tail probability:

$$S_{\text{IT}}(x) = -\log P(\tau(X) \geq \tau(x)) \quad (8)$$

where $\tau : \mathcal{X} \rightarrow \mathbb{R}$ is a feature function (e.g., z-score) and P is the reference distribution.

Given k reference observations $\{x_1, \dots, x_k\}$ from the normal operating period, the empirical IT-score is:

$$\hat{S}_{\text{IT}}(x) = -\log \frac{|\{i \in [k] : \tau(x_i) \geq \tau(x)\}|}{k} \quad (9)$$

where $[k] = \{1, \dots, k\}$.

Theorem C.1 (IT-Score Saturation). *Let \hat{S}_{IT} be the empirical IT-score with k reference observations. Then:*

1. **Upper bound:** $\hat{S}_{\text{IT}}(x) \leq \log k$ for all x .
2. **Saturation:** If $\tau(x) > \max_{i \in [k]} \tau(x_i)$, then $\hat{S}_{\text{IT}}(x) = \log k$ (or $\approx \log(2k)$ with Laplace smoothing).
3. **Non-injectivity:** For multiple observations $x^{(1)}, \dots, x^{(m)}$ all exceeding the reference maximum, $\hat{S}_{\text{IT}}(x^{(j)})$ is identical for all $j \in [m]$.

See Appendix A for the proof.

Corollary C.2 (IT-Scores are Non-Injective Under Saturation). *When multiple post-fault observations exceed the reference distribution (i.e., $\tau(x^{(j)}) > \max_{i \in [k]} \tau(x_i)$ for $j = 1, \dots, m$), the empirical IT-score fails to be injective, assigning identical scores to observations with potentially vastly different deviation magnitudes.*

Theorem C.3 (Counterexample to Marginal Score Ordering). *There exist systems where faults propagate through external properties such that the root cause component does not have the highest marginal anomaly score S^E . See Appendix A for the proof.*

Corollary C.4 (Deviation-Based Scores Enable RCA). *Under the assumption that the root cause component has a distinct deviation magnitude from all other components, deviation-based scores (z-score, IQR-score, MAD-score) can correctly identify and rank the root cause. See Appendix A for the proof.*

Corollary C.5 (IT-Scores Fail for RCA Under Saturation). *When a fault causes multiple components to exhibit anomalies exceeding their historical bounds (a common scenario in distributed systems where faults propagate), IT-scores assign identical scores to all affected components, preventing reliable root cause identification. See Appendix A for the proof.*

D. Internal-External Property Labeling

D.1. Theoretical Foundation

This section provides theoretical grounding for the internal-external property classification. The distinction between internal and external properties aligns with established observability frameworks in distributed systems, as in Li et al. (2022) and the Google SRE golden signals (Google, 2024). We classify properties as:

- ▷ **External properties** (Quality-of-Service metrics): Observable outcomes at service boundaries that other components can detect through interactions, including response time, duration, latency, and error rate.
- ▷ **Internal properties** (Resource metrics): Local component states not directly observable by other components. Examples: CPU usage, memory utilization, disk I/O, socket count. The framework extends naturally to other internal data sources, such as log patterns (error counts, exception frequencies, log message anomalies) and trace spans internal to a component (processing durations, retry counts, queue depths), as long as these observables remain local to the component and are not directly visible through inter-component interfaces.

This classification reflects the RED method (Rate, Errors, Duration) for service-level metrics (Wilkie, 2018) and the USE method (Utilization, Saturation, Errors) for resource metrics (Gregg, 2013). The key insight is that external properties represent *what other components observe*, while internal properties represent *why the component behaves that way*.

D.2. Empirical Validation of Axioms

We validate Axioms 2.5–2.6 on the 735 failure cases in the RCAEval benchmark.

D.2.1. AXIOM 2.5: INTRACOMPONENT DIRECTIONALITY

Axiom 2.5 states that internal properties are causal ancestors of external properties within each component. We validate this through temporal precedence analysis. For each failure case, we detect the first post-fault timestamp where the anomaly score (z-score) exceeds a threshold of 3.0 for both internal and external properties at the root cause component. We compute $\Delta t = t_{\text{internal}} - t_{\text{external}}$, where negative values indicate internal anomalies precede external anomalies.

Results. Across 698 cases with detectable anomalies in both property types, internal anomalies precede or equal external anomalies in **60.7%** of cases. Table 15 shows results by fault type. Resource faults (CPU, DISK, MEM, SOCKET) strongly support Axiom 2.5, with 65–77% showing internal-first ordering and median Δt of –4 to –7 seconds. Code-level faults exhibit the strongest internal-first pattern (83.3%), as application bugs directly affect processing logic before observable service degradation. These faults directly affect internal resources before manifesting in service latency. Nevertheless, network faults (DELAY, LOSS) show the opposite pattern as the root cause of network faults is in the network, not the component internal.

Table 15. Temporal precedence analysis by fault type. “Int First” indicates the percentage of cases where internal anomalies precede or equal external anomalies. Negative Δt values confirm internal-first ordering.

Fault Type	n	Int First	Median Δt
<i>Resource Faults</i>			
CPU	117	76.9%	–7.0s
DISK	113	73.5%	–6.0s
MEM	120	65.8%	–4.0s
SOCKET	45	64.4%	–5.0s
<i>Network Faults</i>			
DELAY	113	27.4%	+11.0s
LOSS	109	41.3%	+9.0s
<i>Code-Level Faults</i>			
F1–F4	78	83.3%	–13.0s
Overall	698	60.7%	–4.0s

D.2.2. AXIOM 2.6: INTERCOMPONENT ISOLATION

Axiom 2.6 states that faults propagate between components only through external properties. We validate this by comparing internal scores of root cause versus affected components. For each failure case, we compute S^I for the root cause and all other components. We measure the ratio $S^I(\text{root cause}) / \max_a S^I(C_a)$ where C_a ranges over affected components (those with elevated external scores).

Results. Across all 735 cases, the root cause’s internal score S^I exceeds the maximum internal score among affected components in 66.5% of cases, with a median ratio of $2.73 \times$. The separation is even more pronounced in absolute terms, where the mean root cause S^I reaches 222M compared to only 6.2K for the mean maximum affected S^I . This substantial separation validates that faults manifest internally at the root cause while propagating only through external properties to downstream components.

Figure 6 visualizes this separation. Root cause components (red) appear in the upper-right quadrant with elevated scores in both dimensions. Affected components (gray) primarily cluster along the external axis, reflecting propagated latency/error anomalies without corresponding internal resource anomalies.

D.2.3. SCOPE AND APPLICABILITY OF CPM AXIOMS

The Component-Property Model (CPM) axioms establish a foundation for principled root cause analysis. Rather than rigid requirements, these axioms characterize system architectures where PRISM can be applied with high confidence. This subsection identifies real-world systems satisfying the CPM axioms, discusses deployment scenarios where axioms may not hold, and provides practitioners with a decision framework for assessing PRISM’s applicability to their specific systems.

Systems Satisfying CPM Axioms. Many modern system architectures satisfy Axioms 2.5 and 2.6 by design. These systems enable confident application of PRISM for root cause analysis.

Containerized Microservices with Resource Quotas. Modern container orchestration platforms enforce strict resource isolation through kernel-level mechanisms. Kubernetes (Kubernetes, 2024) uses Linux cgroups to implement CPU and memory limits, ensuring that one pod’s resource consumption cannot directly modify another pod’s internal resource availability. When properly configured, containerized deployments satisfy Axiom 2.6. The RcaeVal benchmark uses such containerized Kubernetes deployments, which explains the strong empirical validation observed in Section D.

Actor Model Systems. Systems based on the actor model exemplify CPM axioms through state encapsulation. Akka (Lightbend, 2024) and Erlang OTP (Erlang, 2024) enforce that each actor maintains private state, modifiable only by that actor. All inter-actor communication occurs through asynchronous message passing, representing external properties and interactions. This architectural constraint ensures that one actor cannot directly affect another’s internal state, satisfying Axiom 2.6. The sequential message processing within each actor provides temporal causality (internal then external), satisfying Axiom 2.5.

Service-Oriented Architecture. SOA principles (Erl, 1900; AWS, 2025b) enforce component isolation through service interfaces. Services interact through explicit contracts, with no access to internal implementation details. This separation of interface from implementation creates boundaries that satisfy Axiom 2.6. Each service’s internal state (e.g., caches, db) remains invisible to other services, while external properties (e.g., response time) propagate through the network.

Serverless with Tenant Isolation. Recent serverless platforms offer explicit tenant isolation modes. AWS Lambda’s tenant isolation feature (AWS, 2025a) creates separate execution environments for each tenant, preventing resource contention and interference. While this trades off cold start overhead for stronger isolation guarantees, it ensures that one tenant’s function execution cannot directly affect another tenant’s internal metrics, satisfying Axiom 2.6.

While many systems satisfy CPM axioms, we can always find a system that does not. The key insight is that CPM

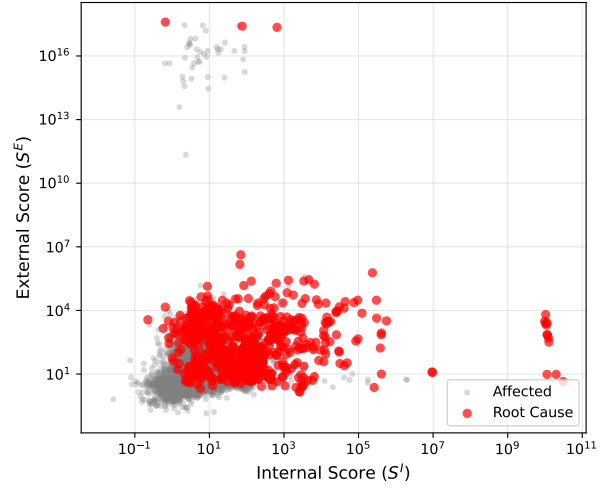


Figure 6. Internal (S^I) vs. external (S^E) scores for all components across 735 failure cases. Root cause components (red) exhibit high scores in both dimensions, while affected components (gray) cluster along the axis with lower internal scores.

axioms characterize a design space where PRISM is most reliable. The practitioners can then decide whether they can apply PRISM into their production with confidence or not.

While CPM axioms provide a foundation for effective RCA, future work can extend PRISM’s applicability and robustness, including: (1) **Evaluation Under Resource Contention.** Test PRISM on over-subscribed Kubernetes clusters where axioms are violated. Establish performance bounds and quantify accuracy degradation when interference exceeds tolerance levels. (2) **Axiom Violation Detection.** Develop diagnostic tests to automatically detect when CPM axioms are violated in production systems, enabling runtime warnings and guiding infrastructure improvements. (3) **Adaptive Property Classification.** Develop methods to automatically classify metrics as internal or external based on system topology and metric semantics, reducing manual labeling burden for new systems. (4) Integrate axiom compliance monitoring with infrastructure management, enabling real-time enforcement of isolation guarantees and automated remediation when violations occur.

E. Reproducibility

We will provide the complete implementation as supplementary material shortly. This section describes how to reproduce all experimental results.

E.1. Environment Setup

```
# Requires Python 3.10+
pip install -e .
```

The code runs on standard hardware (8 CPUs, 16GB RAM). No GPU is required. The complete benchmark using pre-computed results runs in under 5 minutes.

E.2. Reproducing Tables from Pre-computed Results

The `output` / directory contains pre-computed results for all 735 failure cases. The following commands generate the paper tables.

Table 2 (Overall Performance).

```
python run_eval.py \
--methods cholesky baro counterfactual pc_pagerank \
rclagent score_ordering simple_traversal \
smooth_traversal prism \
--sort --ignore-top5 --average-only --ignore-std \
--text-width --pvalue --latex table.tex
```

Expected output: PRISM achieves 68% Top-1, 91% Top-3, 87% Avg@5.

Table 3 (RE2OB Detailed Results).

```
python run_eval.py --filter re2ob \
--methods cholesky baro counterfactual pc_pagerank \
rclagent score_ordering simple_traversal \
smooth_traversal prism \
--sort --ignore-top5 --ignore-std --text-width \
--pvalue --latex table.tex
```

Table 5 (Robustness Analysis).

Anomaly scorers:

```
python run_eval.py --methods prism prism_iqr \
prism_it prism_it_iq --ablation --latex table.tex
```

Pooling strategies:

```
python run_eval.py --methods prism prism_mean \
prism_sum --ablation --latex table.tex
```

Root cause scoring:

```
python run_eval.py --methods prism prism_additive \
--ablation --ignore-std --latex table.tex
```

Table 6 (Ablation Study).

```
python run_eval.py --methods prism_marginal prism \
prism_internal prism_external \
--ablation --latex table.tex
```

Per-Dataset Tables (Appendix C.1).

```
# Replace DATASET with: relob, relss, reltt,
# re2ob, re2ss, re2tt, re3ob, re3ss, re3tt
python run_eval.py --filter DATASET --latex table.tex
```

Figure 3 (Efficiency).

```
python run_eval.py --time \
--efficiency-json efficiency.json
python visualize_box_plot_efficiency.py \
--input efficiency.json \
--output efficiency_boxplot.pdf
```

Figure 4 (Sensitivity).

```
python run_robustness.py --method prism \
--ratio 0.1 0.2 0.3 0.4 0.5 0.6 0.7 0.8 0.9 1.0
python robustness_plot.py
```

E.3. Re-running Experiments from Scratch

To verify results by running all methods from scratch:

```
# Run all methods (approx. 2 hours)
python run_bench.py --methods prism baro pc_pagerank \
cholesky counterfactual score_ordering \
simple_traversal smooth_traversal --force

# Generate evaluation tables
python run_eval.py --latex results.tex
```

Note: RCLAgent requires an OpenAI API key (OPENAI_API_KEY environment variable) and takes several hours due to LLM inference.